Heat-induced changes in the abundance of wheat Rubisco activase isoforms

Gustaf E. Degen[1], Douglas J. Orr[1], Elizabete Carmo-Silva[1,*]

[1] Lancaster Environment Centre, Lancaster University, Lancaster, LA1 4YQ, UK

* For correspondence (Email: e.carmosilva@lancaster.ac.uk; Tel: +44 1524 594369)

ORCID

Gustaf E Degen ID https://orcid.org/0000-0002-0804-4169

Douglas J Orr ID https://orcid.org/0000-0003-1217-537X

Elizabete Carmo-Silva ID https://orcid.org/0000-0001-6059-9359

TWITTER

Gustaf Degen @plantgustaf

Douglas J Orr @SciDoug

Elizabete Camo-Silva @ecarmosilva

Lab @LancsPhotosynth

Department @LancsUniLEC

Total word count for the main body of the text (I, M&M, R, D):	6530
Word count for Introduction:	1365
Word count for Materials and Methods:	1950
Word count for Results:	1489
Word count for Discussion:	1726
Number of figures (all colour):	7
Number of tables:	1
Supporting information figures:	9
Supporting information tables:	5

Summary

- The *Triticum aestivum* (wheat) genome encodes three isoforms of Rubisco activase (Rca) differing in thermostability, which could be exploited to improve the resilience of this crop to global warming. We hypothesised that elevated temperatures would cause an increase in the relative abundance of heat stable Rca1β.
- Wheat plants were grown at 25/18°C (day/night) and exposed to heat stress (38/22°C) for up to 5 days at pre-anthesis. Carbon assimilation, Rubisco activity, CA1Pase activity, transcripts of Rca1β, Rca2β and Rca2α, and the quantities of the corresponding protein products were measured during and after heat stress.
- The transcript of *Rca1β* increased 40-fold in 4 hours at elevated temperatures, and returned to the original level 4 hours upon return of plants to control temperatures. Rca1β comprised up to 2% of the total Rca protein in unstressed leaves, but increased 3-fold in leaves exposed to elevated temperatures for 5 days, and remained high 4 hours post heat stress.
- These results show that elevated temperatures cause rapid changes in *Rca* gene expression and adaptive changes in Rca isoform abundance. The improved understanding of the regulation of carbon assimilation under heat stress will inform efforts to improve wheat productivity and climate resilience.

Running title: Wheat Rca pool composition under heat stress

Keywords: carbon assimilation, crop improvement, food security, heat stress, photosynthesis, Rubisco activase, Rubisco regulation, *Triticum aestivum* (wheat)

Introduction

Wheat production is threatened by the increasing frequency of heat stress in combination with other abiotic factors (IPCC, 2014; Slattery & Ort, 2019; Ray *et al.*, 2019). Field studies show that predicted benefits of increasing atmospheric CO_2 for plant growth are offset by drought and heat stress (Ruiz-Vera *et al.*, 2013; 2015; Gray *et al.*, 2016). Moreover, increases in [CO_2] result in increased canopy temperature (Long *et al.*, 2006). Although plants can cool their leaves by transpiration (Ayeneh *et al.*, 2002), increased drought frequencies limit water availability and increase leaf temperature (Carmo-Silva *et al.*, 2012). As leaf temperature increases, respiration rates increase exponentially while photosynthesis declines above an optimum temperature threshold for each species (Way & Yamori, 2014). Acclimation of respiration to the growth temperature further compounds the balance between the two processes (Atkin *et al.*, 2005). The photosynthetic machinery also adapts to the growth environment (Berry & Bjorkman, 1980; Yamori *et al.*, 2013; Thomey *et al.*, 2019), and depending on the extent of temperature changes, photosynthetic limitations may be reversible or cause permanent damage. Broadening the temperature range for optimal carbon assimilation in wheat is important because global production is predicted to decline in response to rising temperatures (Asseng *et al.*, 2015; Liu *et al.*, 2016).

The activity of ribulose-1,5-bisphosphate (RuBP) carboxylase/oxygenase (Rubisco) has long been identified as the site of heat inactivation of the Calvin-Benson-Bassham Cycle (CBBC) (Weis, 1981). This inactivation is largely due to an inefficient regulation of Rubisco activity by the heat-sensitive molecular chaperone Rubisco activase, Rca (Crafts-Brandner & Salvucci, 2000; Salvucci *et al.*, 2001). Rubisco itself remains active up to 50°C (Salvucci & Crafts-Brandner, 2004b; Galmés *et al.*, 2016), but the reactions it catalyses are differently affected by temperature (Galmés *et al.*, 2019). In addition to CO_2 assimilation by reaction with RuBP, Rubisco can use O_2 as an alternative gaseous substrate, which initiates photorespiration and results in a net loss of CO_2 (Ogren, 1984). Oxygenation occurs at faster rates as temperature increases because the solubility of CO_2 decreases more rapidly than O_2 with temperature (Ku & Edwards, 1977; Bauwe *et al.*, 2010; Dusenge *et al.*, 2019), leading to substantial crop yield losses under future climate scenarios (Walker *et al.*, 2016).

Environmental factors such as [CO_2] and growth temperature have been shown to affect the expression of Rubisco small subunit genes (*RbcS*) in Arabidopsis (Cheng *et al.*, 1998; Yoon *et al.*, 2001; Cavanagh & Kubien, 2013), the relative abundance of RbcS isoforms in rye (Huner & Macdowall, 1979; Huner & Hayden, 1982), and Rubisco properties in spinach (Yamori *et al.*, 2006). Specific residues in the Rubisco large subunit (rbcL) have also been linked to improved catalytic capacity at high temperatures (Prins *et al.*, 2016; Sharwood *et al.*, 2016). Thus, the temperature dependence of Rubisco activity appears to be determined by the inherent properties of the amino acid residues that make up the protein,

and by the combination of rbcL assembled with diverse RbcS isoforms. While phenotypic plasticity enables plants to adapt the photosynthetic machinery to warmer temperatures, short-term heat stress is likely to cause detrimental effects (Leakey *et al.*, 2003).

The regulation of Rubisco activity by Rca is particularly sensitive to temperature (Salvucci *et al.*, 2001; Carmo-Silva & Salvucci, 2011). The active site of Rubisco is prone to deactivation by tight-binding of inhibitory sugar-phosphate derivatives, the production of which increases with temperature (Salvucci & Crafts-Brandner, 2004c; Schrader *et al.*, 2006). Reactivation requires Rca to remodel the active site of Rubisco and facilitate the release of such inhibitors (Salvucci *et al.*, 1985; Bhat *et al.*, 2017). Subsequent removal of a phosphate group from these compounds by specific phosphatases, such as 2-carboxy-D-arabinitol-1-phosphate (CA1P) phosphatase (CA1Pase) and xylulose-1,5-bisphosphate (XuBP) phosphatase (XuBPase), renders them non-inhibitory (Andralojc *et al.*, 2012; Bracher *et al.*, 2015). Overexpression of *ca1pase* decreased Rubisco abundance and grain yields in wheat (Lobo *et al.*, 2019), but the temperature response of the phosphatases that act in concert with Rca to regulate the activity of Rubisco has received little attention to date. On the other hand, the temperature optimum of Rubisco activation by Rca has been shown to follow a pattern that resembles the species adaptation to growth at different temperatures (Carmo-Silva & Salvucci, 2011). In wheat, the optimal leaf temperature for photosynthesis is between 20-25°C (Porter & Gawith, 1999; Silva-Pérez *et al.*, 2017) and decreased capacity for carbon assimilation at elevated temperatures has been linked to the heat sensitivity of Rca (Law & Crafts-Brandner, 2001; Yang *et al.*, 2020).

The potential for greater photosynthetic thermotolerance by improving Rca thermostability has been shown for Arabidopsis (Kurek *et al.*, 2007; Kumar *et al.*, 2009) and rice (Wang *et al.*, 2010; Scafaro *et al.*, 2016; Shivhare & Mueller-Cajar, 2017; Scafaro *et al.*, 2018), making it a promising target for improving photosynthesis at high temperatures in other crops. This could be achieved by exploiting natural diversity in species adapted to warm environments. Light activation of Rubisco by Rca was inhibited by moderately high temperatures to a greater extent in wheat than in heat-tolerant cotton (Feller *et al.*, 1998; Law *et al.*, 2001). In two wild rice species, higher capacity for Rubisco activation at high temperatures resulted in photosynthetic thermotolerance (Scafaro *et al.*, 2012), and was associated with improved Rca thermostability compared to cultivated rice (Scafaro *et al.*, 2016). Heat stress was also shown to increase abundance of the large Rca isoform in domesticated rice, with plants overexpressing this isoform having increased seedling aboveground biomass dry weight when exposed to heat stress (Wang *et al.*, 2010).

Wheat contains two Rca genes as do the majority of grass species, with exceptions including rice where the *OsRca1* gene is thought to be non-functional (Nagarajan & Gill, 2018). Wheat *Rca1* produces a 42.9 kDa Rca1β isoform and *Rca2* produces a 42.3 kDa

Rca2β and a 46.2 kDa Rca2α isoform via alternative splicing (Carmo-Silva *et al.*, 2015). Recent detailed analyses of the temperature response of wheat Rca isoforms showed that Rca1β is more thermostable than Rca2β and Rca2α (Scafaro *et al.*, 2019; Degen *et al.*, 2020). However, Rubisco activation by Rca1β is relatively inefficient at elevated temperature, due to high rates of ATPase activity in relation to Rubisco activation (Degen *et al.*, 2020). Gene expression of *Rca1β* increased by varying extents in two wheat cultivars exposed to short-term (2 days) heat stress at two growth stages (Scafaro *et al.*, 2019). Rca protein abundance may also be regulated post-transcriptionally as suggested by the observation of a decrease in total *Rca* transcript accompanied by an apparent increase in total Rca protein abundance under short-term heat stress (2 days; Law & Crafts-Brandner, 2001). Wheat leaves developed under longer-term heat stress (2 weeks) showed no significant change in Rca protein abundance, but Rcaβ was more abundant in leaves that were simultaneously exposed to drought and heat (Perdomo *et al.*, 2017). Importantly, studies to date did not distinguish between the abundance of the two short protein isoforms, Rca1β and Rca2β, which have similar molecular weights (Carmo-Silva *et al.*, 2015), but differ in heat sensitivity (Scafaro *et al.*, 2019; Degen *et al.*, 2020).

A detailed understanding of the temperature response of Rubisco regulation will become increasingly important with predictions of increased frequency of future heat waves (Slattery & Ort, 2019) and more variable leaf temperatures (Vico *et al.*, 2019). Given the previously characterised differences in the temperature response of Rubisco activation by wheat Rca isoforms (Degen *et al.*, 2020), here we set out to investigate how whole-plant heat stress impacts Rca protein levels. Specifically, we tested the hypothesis that the relative abundance of wheat Rca isoforms would change so that leaves of heat-stressed plants contain relatively more of the thermostable Rca1β, and these changes would be accompanied by altered photosynthetic biochemistry, physiology and grain yield. This was tested by exposing plants to a five-day period of heat stress at pre-anthesis (a critical stage of wheat plant development). Net CO_2 assimilation, Rubisco activity and abundance, CA1Pase activity, and the abundance of the three Rca isoforms were determined during and immediately after heat stress. Findings are interpreted in relation to the thermostability of wheat Rca isoforms and will inform approaches to improve photosynthetic regulation under increasingly warm and variable temperatures for enhanced crop productivity and resilience to climate change.

Materials and Methods

Plant growth and heat stress conditions

Triticum aestivum L. cv. Cadenza seeds were soaked in de-ionised H_2O for 24h at 7°C prior to sowing in a wheat mix growth medium (Petersfield compost, Hewitt & Son Ltd., Cosby, UK). Twenty plants per experiment were grown in a heated glasshouse for three weeks in 3 L pots before being divided into two groups and transferred to two controlled environment cabinets (Snijders Labs, Tilburg, Netherlands). Cabinets were set to 25/18°C day/night, with a 16 h photoperiod, photosynthetic photon flux density (PPFD) at the plant level of 450 µmol m^{-2} s^{-1}, and 60% relative humidity until the flag leaf of the main tiller was fully expanded (approximately 3 weeks). For the heat stress treatment, once the flag leaves were visible, the temperature in one of the two cabinets was raised to 34/22°C day/night for one day, followed by five days at 38/22°C day/night (Fig. **1a**). Night-time warming causes increased dark respiration (e.g. Rashid *et al.*, 2020) and decreased yields of crops such as wheat and rice (Sadok & Jagadish, 2020). Effects on productivity are complex, genotype-specific, and may be more pronounced when night-time elevated temperatures occur at the reproductive stage (Hein *et al.*, 2019; Impa *et al.*, 2019) compared to earlier growth stages (Frantz *et al.*, 2004; Peraudeau *et al.*, 2015). In the present study, both day- and night-time temperatures were increased in the heat stress cabinets to replicate real-world conditions, and measurements were taken during the day focusing on photosynthetic traits. After 5 days at 38/22°C, the cabinet was returned to control temperatures (25/18°C) at the end of the photoperiod on experiment day 7. Temperatures in each cabinet were increased over the course of 1 h at the start of the photoperiod and decreased over the course of 1 h at the end of the photoperiod. Air temperature and relative humidity in each cabinet were measured continuously during the course of the heat stress treatment (OM-EL-USB temperature and humidity data logger, Omega Engineering, UK; Fig. **1b**, Fig. **S1**).

Two consecutive experiments were completed switching the cabinets used for control conditions and the heat stress treatment. In each experiment, a set of 5 plants (i.e. 10 plants in total for control and 10 plants in total for heat stress) was used for non-destructive repeated measures of *in vivo* gas-exchange over the course of the heat stress treatment. This same set of plants was used for final biomass and grain yield. A separate set of 4 plants per experiment (i.e. 8 plants in total for control and 8 plants in total for heat stress) was used for collecting samples for biochemical analysis.

Measurements and samples were taken at four time-points during the experiment: (1) the day prior to the start of the heat treatment, corresponding to experiment day 1, when all plants were exposed to control conditions; (2) four hours and (3) five days into the heat stress exposure period, corresponding to experiment days 3 and 7, when plants were either exposed to control or elevated temperatures; and (4) the day after the end of the heat

196 treatment, when plants were exposed to control conditions to assess recovery from heat
197 stress, corresponding to experiment day 8 (Fig. **1a**). No samples or measurements were
198 taken on the other days of the experiment.
199 Samples were collected 4 hours into the beginning of the photoperiod and *in vivo*
200 measurements were taken 5-6 hours into the photoperiod. At each of the four time-points,
201 samples for biochemistry were taken from a flag leaf in a separate tiller of each plant
202 (repeated sampling from each biological replicate throughout the experiment). Leaf segments
203 of known area were immediately snap frozen in liquid nitrogen and kept at -80°C until
204 analysis. Sampling for biochemistry resulted in approximately half of the flag leaf being
205 removed from the sampled tiller and each plant contained on average 15 fertile tillers.
206 Measurements and sampling were always taken from flag leaves of tillers at the booting
207 stage, i.e. prior to ear emergence. Leaf temperature was measured before sampling using a
208 thermocouple (CDH-SD1, Omega Engineering, UK; Fig. **1c**) and light level was measured
209 with a PAR meter (MQ-200, Apogee Instruments, Canada).
210
211 Gas-exchange measurements
212 Steady-state measurements of net CO_2 assimilation (A) and stomatal conductance to water
213 vapour (g_s) used an open gas-exchange system (LI-6400XT, Li-COR, Lincoln, NE, USA) at a
214 PPFD of 400 µmol m^{-2} s^{-1}, a reference CO_2 concentration of 400 µmol mol^{-1} and a flow rate of
215 300 µmol s^{-1}. The gas-exchange system was placed inside the respective growth cabinets,
216 under control or heat stress conditions. The temperature of the block in the leaf chamber was
217 set to 25°C for plants in the control cabinet and to 38°C for plants in the heat stress cabinet
218 (experiment days 3 and 7). The water vapour pressure deficit (VPD) was maintained at 1-1.6
219 kPa by adjusting the humidity inside the leaf chamber of the gas-exchange system as
220 needed, and calculated from the leaf temperature during gas-exchange measurements.
221
222 Gene expression analyses
223 Gene expression of *ca1pase, Rca1β, Rca2β+α, Rca2α, RbcS1-25* and *rbcL,* were
224 determined by reverse-transcription quantitative PCR (RT-qPCR). mRNA was extracted from
225 plant tissue using a NuceloSpin® Tri Prep kit (Macherey-Nagel, Düren, Germany), including
226 a DNase treatment. mRNA yield and purity were assessed using a spectrometer by
227 measuring absorbance at 230, 260 and 280 nm (SpectroStar Nano, BMG Labtech GmbH,
228 Ortenberg, Germany). cDNA synthesis used 1 µg mRNA and the Precision nanoScript™ 2
229 Reverse Transcription kit (Primer design Ltd., Camberley, UK). qPCR reactions used 40 ng
230 of cDNA and the primer pair for the target gene in a Mx3005P qPCR system (Stratagene,
231 Agilent Technologies, Stockport, UK). RT-qPCR details including cycle conditions are
232 described in the MIQE checklist (Table **S1**). *Ta2291* (ADP-ribosylation factor) and *Ta2776*

(similar to RNase L inhibitor-like protein) were used for normalisation due to their high expression stability across various environmental conditions (Paolacci *et al.*, 2009). Primer efficiency for each primer set was analysed according to Pfaffl *et al.* (2001). Primers were designed to bind to all three sub genomes (Table **S2**), except for *rbcL*, which is encoded in the chloroplast genome. Primers for *Rca2* amplified both splicing products. EnsemblPlants was used to search for genes annotated as *RbcS*; 25 genes were identified and divided into three groups according to the similarity of the respective protein sequences (Table **S3**). Primer pairs were designed to quantify the expression of each of the three *RbcS* groups (Table **S2**).

Enzyme activity assays

Photosynthetic proteins were extracted essentially as described by Carmo-Silva *et al.* (2017) with slight modifications, as follows. Leaf samples were ground using an ice-cold mortar and pestle containing 0.8 mL of (final concentrations) 50 mM Bicine-NaOH pH 8.2, 20 mM $MgCl_2$, 1 mM EDTA, 2 mM benzamidine, 5 mM ε-aminocaproic acid, 50 mM 2-mercaptoethanol, 10 mM dithiothreitol, 1% (v/v) plant protease inhibitor cocktail (Sigma-Aldrich Co., St Louis, MO, USA), and 1 mM phenylmethylsulphonyl fluoride.

Rubisco activity was determined by incorporation of $^{14}CO_2$ into acid-stable products at 30°C (Parry *et al.*, 1997; Carmo-Silva *et al.*, 2017) in reaction mixtures containing (final concentrations) 100 mM Bicine-NaOH pH 8.2, 20 mM $MgCl_2$, 10 mM $NaH^{14}CO_3$ (9.25 kBq μmol^{-1}), and 0.6 mM RuBP (added to tubes individually). Initial activity assays started with leaf extract addition, while total activity assays started with RuBP addition after allowing carbamylation of Rubisco for 3 min. Reactions were quenched after 30 s with 4N formic acid, then dried, rehydrated with de-ionised H_2O, mixed with scintillation cocktail (Gold Star Quanta, Meridian Biotechnologies, Epsom, UK) and subject to liquid scintillation counting (Packard Tri-Carb, PerkinElmer). Rubisco activation state was calculated from the ratio of initial/total Rubisco activity. Rubisco amounts were determined by a [^{14}C]carboxyarabinitol-1,5-bisphosphate (^{14}C-CABP) binding assay (Whitney *et al.*, 1999).

CA1Pase activity was measured according to Lobo *et al.* (2019) and Andralojc *et al.* (2012) in reaction mixtures (90 µL) containing (final concentrations) 50 mM BisTrisPropane-HCl pH 7.0, 200 mM KCl, 1 mM EDTA, 1 mM ε-aminocaproic acid, 1 mM benzamidine, 10 mM $CaCl_2$, 0.5 mg mL^{-1} BSA and 1% (v/v) protease inhibitor cocktail. For each sample, two technical replicates containing 0.5 mM 2-carboxy-D-ribitol-1,5-bisphosphate (CRBP, a substrate for CA1Pase) and two replicates without CRBP were prepared, in addition to a blank containing no leaf extract. Reactions were initiated by adding 5 µL of leaf extract and quenched after 60 min at 22°C in a temperature-controlled dry bath (Echotherm, Torrey Pines Scientific, USA) by adding 30 µL of 1 M trichloroacetic acid. Reactions were

centrifuged for 3 min at 14,000 *g* to sediment BSA, then 100 µL of supernatant was transferred into a microplate well to determine inorganic phosphate by adding 200 µL of 2.2% (w/v) ammonium molybdate in 1.6 M H_2SO_4, incubating 10 min, adding 50 µL of 0.035% (w/v) malachite green in 0.35% (w/v) polyvinyl alcohol, incubating 60 min at room temperature, and measuring absorbance at 610 nm. Inorganic phosphate in the samples was calculated from a standard curve of 0-10 nmol KH_2PO_4.

Gel electrophoresis and immunoblotting

Total soluble proteins (TSP) in leaf extracts were quantified by the Bradford method (Bradford, 1976), then separated by sodium dodecyl sulfate polyacrylamide gel electrophoresis (SDS-PAGE) followed by immunoblotting, essentially as described by Perdomo *et al.* (2018). A primary antibody anti-Rca produced in rabbit against cotton Rca (Salvucci, 2008) was used for quantification of all Rca α and β isoforms using 2 µg TSP per sample. A primary polyclonal antibody that specifically detects the wheat Rca1β isoform was produced in rabbit (Cambridge Research Biochemicals Ltd., Cleveland, UK) using a short peptide at the N-terminal region where the protein differed sufficiently from Rca2β (KKELDEGKQTNADR, corresponding to residues 3-16 of the mature sequence, Fig. **S2**). Detection of Rca1β required the use of 6 µg TSP per sample. A dilution series of 20, 50 and 100 ng purified recombinant Rca2β+α at a 90:10 ratio was added to each gel for quantification of total Rca α and β isoforms; and a dilution series of 1, 5 and 20 ng purified recombinant Rca1β was added to each gel for quantification of Rca1β (Fig. **S2**). Recombinant Rca proteins used for standards were purified as described in Barta *et al.* (2011). A fluorescent secondary antibody (anti-rabbit, 800CW, Li-COR Biosciences) was used to detect Rca by imaging blots at 800 nm using an Odyssey system (Li-COR Biosciences, Lincoln, NE, USA). Protein levels were calculated from the standard curves of purified Rca. Quantities of Rca2β were calculated by subtracting Rca1β from the total Rca β isoform.

Biomass and yield traits

After the heat stress treatment, at the end of experiment day 8, plants were transferred back into the glasshouse and kept well-watered until reaching full maturity. Aboveground biomass and grain yield traits were determined for each plant as described by Lobo *et al.* (2019).

Statistical analysis

Significance of differences between control and heat stress plants was analysed using Restricted Maximum Likelihood (REML), which gives the same *P* values and multiple comparisons tests as repeated measures ANOVA. The mixed model was fitted in GraphPad

Prism 8 using the Geisser-Greenhouse correction to account for possible violations of sphericity. The lack of significant differences in biochemical (destructive flag leaf sampling) and physiological (non-destructive flag leaf sampling) traits between control plants analysed at different time-points suggests that repeated sampling caused no significant wounding effect on Rca gene expression and protein levels in flag leaves from adjacent tillers. Significance of differences in grain yield and biomass between treatments was assessed by two-sided t-tests with alpha set to 0.05 using R (version 3.6.0; R Core Development Team, 2013) and RStudio (version 1.2.5001; R Studio Team, 2019). Box and whiskers plots were prepared using ggplot2 (Wickham, 2017); boxes show medians and first and third quartiles (25^{th} and 75^{th} percentiles), and whiskers extend from the hinge to the largest or smallest value. Symbols represent individual data points and black diamonds represent the mean values. Plants in the two cabinets on the day prior to the onset of heat stress (i.e. under control conditions) were not statistically different in their rates of CO_2 assimilation or Rubisco properties and were combined for data analysis (Table **S4**).

Results

Wheat plants were exposed to heat stress conditions over a period of 5 days before reaching anthesis (booting stage) in a pot experiment and using plant growth cabinets for environmental control. The air temperature in the control cabinet corresponded with the set temperatures of 25/18°C, while the day temperature in the heat stress cabinet was slightly below the setting of 38/22°C (Fig. **1a, b**). Leaf temperature (T_{leaf}) was measured to assess the extent to which plants experienced heat stress. Plants in the control cabinet had mean T_{leaf} of 22.5°C and plants in the heat stress cabinet had mean T_{leaf} of 28.7°C, corresponding to a difference between air temperature (T_{air}) and T_{leaf} of 2.5°C for control and 9.3°C for heat stress plants (Fig. **1c**). Plants were maintained well-watered and in a humid environment (Fig. **S1**) throughout the experiment, which would have enabled the greater extent of evaporative cooling during heat stress (Carmo-Silva *et al.*, 2012). Once T_{air} returned to control values on experiment day 8, T_{leaf} in the heat stress cabinet (22.6°C) was again comparable to control plants.

In order to assess the effect of heat stress on carbon assimilation, gas exchange measurements were taken under steady-state conditions resembling those used for plant growth, i.e. a PPFD of 400 µmol m^{-2} s^{-1} and 25°C for control or 38°C for heat stress plants (Fig. **2**). Net CO_2 assimilation (A) in the wheat flag leaves remained unchanged throughout the experiment days for control plants but decreased significantly in plants measured after 4 h of heat stress. The decline in A was greater after 5 days of heat stress, and still observed after the cabinet temperature was returned to control levels (4 h of recovery at control temperatures; Fig. **2a**). Stomatal conductance to water vapour (g_s) was highly variable but remained unchanged in control plants and after 4 h of heat. However, g_s was reduced after 5 days of heat stress and remained significantly lower after 4 h of recovery compared to control plants (Fig. **2b**). Despite attempts to maintain constant cabinet humidity, the vapour pressure deficit based on leaf temperature (VPD_L) increased after 5 days of heat stress compared to control conditions (Fig. **2c**). The intercellular CO_2 concentration did not decrease in response to heat stress, in fact after 4 h of heat there was a slight increase relative to the values prior to heat stress (Fig. **2d**), likely as a result of decreased assimilation (Fig. **2a**).

After the heat stress exposure, all plants were transferred to the glasshouse until maturity to determine the effect of the 5 days heat stress exposure during booting on final biomass and grain yield. Aboveground biomass at 100% dry matter (DM) showed no significant difference between control and heat stress plants (Table **1**). However, the grain weight per plant at 85% DM was significantly lower in plants exposed to the heat treatment. The number of spikes per plant remained constant, suggesting that grain weight per spike was negatively impacted by the heat stress exposure pre-anthesis.

To investigate the impact of heat stress on the regulation of Rubisco activity, flag leaf samples of plants in the control and heat conditions were taken prior to, during, and after the exposure to stress. Initial and total activities and content of Rubisco were not significantly affected during heat stress (Fig. **3**), but total activity and Rubisco content declined slightly in recovery plants on experiment day 8 compared to control plants on experiment day 1 (Fig. **3b, c**, $P = 0.0062$ and $P = 0.0451$, respectively). When expressing the activities of Rubisco per quantity of enzyme (specific activities), no significant differences were observed throughout the experiment (Fig. **S3**). The same was largely true for total soluble protein (TSP), Rubisco content as a fraction of TSP (Fig. **S3**), and chlorophyll a, chlorophyll b and total carotenoids (Fig. **S4**).

Initial and total activities were used to calculate Rubisco activation states (Fig. **3d**), which declined significantly after 4h of heat stress ($P = 0.0006$) but showed no significant difference to control after 5 days of heat stress ($P > 0.05$). Rubisco activation state increased after 4h of recovery on experiment day 8, compared to control plants at the start of the experiment ($P = 0.0014$) and to heat stress plants on experiment day 3 ($P = 0.0044$).

The activation state of Rubisco reflects the balance between inhibition due to binding of inhibitors to active sites, and activation via removal of such inhibitors by Rca and subsequent dephosphorylation of inhibitors by enzymes such as CA1Pase. The activity of CA1Pase remained constant in control plants throughout the experiment, showed a mild, non-significant increase after 5 days of heat stress and was significantly increased in recovery plants post heat stress, on experiment day 8 (Fig. **4**; $P = 0.0442$). These results suggest increased capacity to dephosphorylate sugar-phosphate derivatives that would otherwise inhibit Rubisco activity upon stress relief.

Wheat Rca isoforms differ in their regulatory and thermal properties (Scafaro *et al.*, 2019; Perdomo *et al.*, 2019; Degen *et al.*, 2020). Wheat flag leaves presented very little Rca1β protein compared to both Rca2β, which was most abundant, and Rca2α (Fig. **5**). The amount of Rca1β remained similar to control levels after 4 h of heat stress, but after 5 days of heat stress (68 h of cumulative heat), Rca1β protein levels increased ca. 2.5-fold, and remained at this level the day after heat stress (4 h of recovery at control temperatures). Rca2β and Rca2α abundance remained similar between control and heat stress. The relative abundance of each wheat Rca isoform in the flag leaf highlighted that under control conditions Rca1β was only 1% of the total Rca pool, and that Rca2β was the most abundant isoform corresponding to more than 85% of the total Rca pool (Fig. **6**). The relative abundance of Rca2α appeared to decline slightly as the leaves aged (from experiment day 3 to experiment day 8), but this was not significant ($P > 0.05$). While the total Rca pool size (ca. 6.5 ± 0.9 mg m^{-2}) was unaffected by heat stress, the relative abundance of Rca1β increased from 1% in leaves under control conditions to 6% after 5 days of heat stress (Fig. **6**, Fig. **S5**).

The abundance of Rubisco active sites relative to total Rca monomers ($R_{A.S.}$:Rca_{total}) in wheat flag leaves did not change significantly throughout the experiment and remained at 103 ± 11 mol $R_{A.S.}$ mol^{-1} Rca_{total} (Table **S5**). Because of the increase in Rca1β abundance during heat stress, the abundance of $R_{A.S.}$:Rca1β decreased ca. 5-fold under heat stress.

The timing of changes in *Rca* gene expression during and post heat stress was investigated to assess whether gene expression might contribute to explain the observed changes in relative abundance of the three isoforms. Control plants showed virtually no expression of *Rca1β*, whereas heat-stressed plants showed a ca. 40-fold increase in *Rca1β* expression after 4 h of heat (Fig. **7**). *Rca1β* expression was still increased relative to control plants after 5 days of heat stress exposure, and decreased to near-control levels the day after heat stress. By comparison, expression of the Rca2 gene splice variants *Rca2β* and *Rca2α* showed less clear changes in response to heat stress. To investigate the possibility that heat responsive elements could be driving the change in *Rca1β* expression in response to heat stress, the promoter regions of *Rca* were investigated for presence of such elements based to consensus sequences identified by Jung *et al.* (2013). This revealed the presence of a heat responsive element upstream of *Rca1* genes in all three genomes and interestingly also upstream of the *Rca2* gene copy in the A genome only (Fig. **S6**).

The expression of other genes related to Rubisco function was investigated after 5 days of heat stress exposure only (experiment day 7; Fig. **7**). Despite some heat stress plants showing higher values of *rbcL* expression, there were no significant differences in the expression of *ca1pase*, *rbcL* or *RbcS* genes between control and heat stress plants. The wheat genome encodes at least 25 *RbcS* genes (Table **S2**), which were divided into three groups based on sequence similarity (Fig. **S7**, Table **S3**). The relative expression of *RbcS G2* and *G3* was 4-fold higher than *G1*, and none of the groups showed changes in expression in response to heat stress. Based on data available in the gene expression atlas expVIP (Borrill *et al.*, 2016; Ramirez-Gonzalez *et al.*, 2018), *RbcS G3* appears to be the *RbcS* group most consistently highly expressed in all wheat plant organs, including roots, and across different plant developmental stages and growth conditions (Fig. **S8**). Interestingly, the predicted wheat RbcS G3 protein sequences share an isoleucine residue with the unusual T-type *RbcS1* variant from rice (Morita *et al.*, 2014; Pottier *et al.*, 2018), while the other wheat and rice RbcS isoforms share a valine in the same residue position (Fig. **S9**). The functional significance of this isoleucine residue and potential significance of RbcS presence in non-photosynthetic tissue could warrant further study.

Discussion

Rubisco activation is sensitive to moderate heat stress due to the thermolabile nature of Rca (Salvucci *et al.*, 2001; Salvucci & Crafts-Brandner, 2004a,c; Scafaro *et al.*, 2012; 2016; Shivhare & Mueller-Cajar, 2017; Degen *et al.*, 2020). In wheat, the isoform Rca1β has recently been shown to be more thermostable than the other two native isoforms, Rca2β and Rca2α (Scafaro *et al.*, 2019, Degen *et al.*, 2020). Here, pre-anthesis heat stress promoted a rapid increase in gene expression and a longer-term adaptive increase in protein abundance of Rca1β compared to the less thermostable wheat Rca isoforms.

Wheat plants exposed to 38°C during the day had leaf temperatures around 28°C and showed a large (40-fold) increase in *Rca1β* expression after 4 h heat stress, with expression remaining high after 5 days heat stress. These findings agree with previous studies in wheat (Law & Crafts-Brandner, 2001; Scafaro *et al.*, 2019). In cotton, there were no significant changes in either mRNA or protein levels of constitutive Rcaβ or Rcaα isoforms, but an additional Rca isoform was found to account for 5% of the total Rca pool after 2 days heat stress (Law *et al.*, 2001). These findings suggest that synthesis of heat-inducible isoforms of Rca may occur and be wide-spread among plant species. The promoter region of the wheat gene *Rca1* contains a heat responsive element in all three genomes, whilst this is only present in the A genome for *Rca2*. These regions have been associated with increased *Rca* expression under heat stress in Arabidopsis (Jung *et al.*, 2013), and are likely related to the increased *Rca1β* expression in wheat.

Rca1β protein abundance did not increase significantly at the onset of heat stress (4 h), but increased 3-fold after 5 days heat stress. Young wheat plants at the 3rd leaf stage showed increased abundance of the 42 kDa protein (Rca1β+Rca2β) after 24-48 h exposure to a 38/34°C day/night heat stress (Law & Crafts-Brandner, 2001). The relative abundance of Rca1β and Rca2β was not assessed in that study, and was only assessed after 4 h and 5 days heat stress in the present study. Further research is required to test whether abundance of thermostable Rca1β protein in wheat increases within 24 h of exposure to heat stress during the day and/or in response to elevated temperatures during the night. The observed response might also differ between cultivars and wheat growth stages (Scafaro *et al.*, 2019). The much larger fold-change in Rca abundance at the transcript level compared to the protein level shows that gene expression and protein abundance are not directly coupled, and suggest that Rca protein abundance might be regulated by a post-transcriptional mechanism (Law & Crafts-Brandner 2001; Law *et al.*, 2001). Understanding such regulatory mechanisms warrants further investigation to inform efforts aimed at optimising Rca levels and Rubisco activation *in planta*.

Leaf temperatures in plants experiencing heat stress (Fig. **1c**) closely matched the temperature optimum for Rubisco activation by Rca1β *in vitro*, whereas in control plants leaf

temperatures approximated those at which Rca2β and Rca2α are most active *in vitro* (Degen *et al.*, 2020). The activation state of Rubisco was lower after 4 h heat stress compared to control plants analysed on the same day, but after 5 days heat stress was not significantly different from control plants. It is possible that the increase in the abundance of the thermostable Rca1β protein contributed to maintaining Rubisco activity during heat stress. It has recently been shown that while Rca2β and Rac2α become unable to activate Rubisco at moderately high temperatures (Scafaro *et al.*, 2019; Degen *et al.*, 2020), Rca1β continues to operate at higher temperatures, but is relatively inefficient compared to the other two isoforms. An increase in Rubisco activation state was observed in both control plants and heat-stressed plants at the end of the experiment (following a 4 h recovery period under control conditions). As the wheat flag leaves age, decreasing Rubisco abundance can be accompanied by an increase in Rubisco activation state (Carmo-Silva *et al.*, 2017). In addition, increased Rubisco activation in recovery plants could also be partly explained by the increase in CA1Pase activity, decreasing the abundance of Rubisco inhibitors.

The properties of a particular Rca isoform can impact the overall properties of the Rca holoenzyme composed of a mixture of isoforms, both *in vitro* and *in vivo* (Zhang *et al.*, 2001; 2002). Scafaro *et al*. (2019) showed that the effects of mixing wheat Rcaβ isoforms *in vitro* were strongly temperature-dependent. At leaf temperatures up to ca. 30°C, it is possible that the small increase in the relative abundance of Rca1β in wheat flag leaves observed in the present study could confer stability to the Rca holoenzyme during heat stress. Testing this hypothesis more thoroughly warrants further detailed study as it raises the possibility that the combination of Rca isoforms present in the leaf might be adjustable to maximise overall efficiency of Rubisco activation in wheat. Importantly, our previous *in vitro* study highlighted that the two activities of Rca have different temperature optima, with fast rates of ATP hydrolysis continuing well above the moderately high temperatures that cause a 50% decrease in Rubisco activation rates (Degen *et al.*, 2020). ATP levels do not decrease under heat stress (Schrader *et al.*, 2004) and the ability of Rca to continue hydrolysing ATP above 30°C may act as a significant ATP sink during heat stress, contributing to prevent irreversible damage of thylakoid membranes (Sharkey & Zhang, 2010).

Catalytic misfire events by Rubisco increase with temperature, resulting in increased production of inhibitory sugar-phosphate derivatives (Schrader *et al.*, 2006; Parry *et al.*, 2008). *In vitro* inhibition of Rubisco by these compounds, termed fallover (Edmondson *et al.*, 1990), declines at high temperature due to a more flexible active site (Schrader *et al.*, 2006; Parry *et al.*, 2008). *In planta*, accumulation of these inhibitors is thought to occur under heat stress due to increased proportion of oxygenation to carboxylation and increased misfire events. Inhibitors that accumulate during heat stress may still be present in increased levels after plants are returned to control conditions, potentially preventing rapid recovery of

Rubisco activity. CA1Pase metabolises sugar-phosphate derivatives (Andralojc *et al.*, 2012), and there was significantly more CA1Pase activity in wheat the day after heat stress compared to plants that did not experience heat stress, suggesting up-regulation of the capacity to restore Rubisco activity for continued carbon assimilation upon relief from stress.

In addition to regulation by Rca and CA1Pase, variations in Rubisco subunit composition have been proposed as a mechanism for adaption to growth temperature (Yoon *et al.*, 2001; Yamori *et al.*, 2006; Cavanagh & Kubien, 2013). Although expression of *rbcL* and *RbcS* groups was not significantly different between plants exposed to control temperatures and heat stress, there was a trend for increased expression of *rbcL* and decreased expression of *RbcS G2* and *G3* under heat stress. These trends might become significant in wheat plants exposed to prolonged heat stress, and could result in altered Rubisco catalytic properties, as shown by Yamori *et al.* (2006). Rubisco is highly abundant (Ellis, 1979; Carmo-Silva *et al.*, 2015; Lobo *et al.*, 2019) and constituted 30-40% of the total soluble protein in the flag leaf of the wheat plants studied here. Therefore, variation in Rubisco subunit composition is likely to be a long-term adaptation response, in part because of the large amount of protein synthesis required. Changes in Rca and CA1Pase activity, on the other hand, could be regarded as a shorter-term mechanism for mitigating the impact of heat stress and maintaining Rubisco functionality.

Carbon assimilation decreased throughout heat stress exposure, and remained low the day after heat stress, which was accompanied by reduced stomatal conductance, in line with previous reports (Law & Crafts-Brandner, 1999; Galmés *et al.*, 2007; Silva-Pérez *et al.*, 2017; Lawson & Vialet-Chabrand, 2018). The intercellular CO_2 concentration (Ci) remained above 250 μmol mol^{-1} throughout the experiment, which is well above the level thought to promote Rubisco decarbamylation and consequent inactivation (Galmés *et al.*, 2010). At high light, the transition of photosynthetic limitation by Rubisco activity to electron transport (and RuBP regeneration) has been reported to occur at Ci values around 300 μmol mol^{-1} (Silva-Pérez *et al.*, 2017). At a non-saturating PPFD of ~400 μmol mol^{-1}, used for both plant growth and gas-exchange measurements in this study, photosynthesis would be more likely limited by the rate of RuBP regeneration than by Rubisco activity (Lauerer *et al.* 1993, von Caemmerer 2000). The large decrease in A observed under heat stress cannot be directly compared to the observed effect of heat stress on productivity traits or Rubisco biochemistry, since gas-exchange was measured at a higher leaf temperature (ca. 37.1°C) than the leaf temperature of plants during the heat stress treatment (ca. 28.7°C).

The 5-day heat stress treatment pre-anthesis significantly decreased plant grain weight at full maturity; a similar impact on grain yield was reported in wheat plants exposed to 5 days heat stress at anthesis (Chavan *et al.*, 2019). These findings support other studies suggesting that flag leaf photosynthesis makes a significant contribution towards grain yield

(e.g. Carmo-Silva *et al.*, 2017). Heat priming wheat plants at pre-anthesis has been shown to result in reduced damage to the flag leaf and increased carbon assimilation in plants exposed to post-anthesis heat stress (Wang *et al.*, 2011). While the priming study was conducted at moderate heat stress (34/30°C day/night for 7 days), it suggests wheat plants can, to some extent, adapt to the growth temperature. However, current evidence and the findings reported herein suggest that isolated events of heat stress affecting flag leaf photosynthetic properties cause a significant decline in wheat productivity.

In summary, the biochemical and molecular responses of pre-anthesis wheat plants exposed to heat stress showed short-term increased gene expression and longer-term increased protein abundance of the more thermostable wheat Rca1β isoform. These findings support previous wheat heat stress reports (Law & Crafts-Brandner, 1999; 2001; Silva-Pérez *et al.*, 2017; Yang *et al.*, 2020) and *in vitro* wheat Rca temperature responses (Scafaro *et al.*, 2019; Degen *et al.*, 2020) suggesting that Rubisco activity and regulation by Rca in wheat are primarily optimised for leaf temperatures between 20-25°C, but with room to improve climate resilience. Manipulation of the relative abundance of Rca isoforms, alongside introduction of superior forms of Rca, through breeding or genetic engineering, offers scope to make Rubisco regulation in wheat more resilient to an increasingly warm and variable climate.

Data availability

The data that support the findings of this study will be openly available in the Lancaster University Research Directory at http://www.research.lancs.ac.uk/portal/en/.

Accession numbers

Wheat Rubisco, Rca, and CA1Pase sequence data can be found in GenBank or EnsemblPlants under accession numbers listed in Supplementary Information Tables **S2**, **S3**.

Acknowledgements

We thank Dr Samuel Taylor for helpful discussion about experimental design and gas-exchange training, Dr Rhiannon Page for help with gene expression analyses, Dr Mike Salvucci for the gift of the anti-Rca antibody and Dr Alejandro Perdomo for help with developing a specific anti-Rca1β antibody. We are also grateful to the reviewers for their useful and productive feedback on the manuscript. This research was supported by a studentship from the Lancaster Environment Centre to GED and by the Biotechnology and Biological Sciences Research Council (BBSRC) through the International Wheat Yield Partnership projects '*Speeding the adjustment of photosynthesis to shade-sun transitions to increase yield potential in the field*' (IWYP163; BB/S005072/1) and '*Manipulating stomatal blue light response in wheat to improve productivity*' (IWYP123; BB/S005080/1) to ECS.

Author contributions

GED, DJO and ECS designed research; GED performed research with help from DJO; GED analysed data; and GED and ECS wrote the manuscript with help from DJO.

Conflicts of interest

The authors declare that they have no conflicts of interest.

References

Andralojc PJ, Madgwick PJ, Tao Y, Keys A, Ward JL, Beale MH, Loveland JE, Jackson PJ, Willis AC, Gutteridge S, *et al.* 2012. 2-Carboxy-D-arabinitol 1-phosphate (CA1P) phosphatase: evidence for a wider role in plant Rubisco regulation. *Biochemical Journal* **442**: 733–742.

Asseng S, Ewert F, Martre P, Rotter RP, Lobell DB, Cammarano D, Kimball BA, Ottman MJ, Wall GW, White JW, *et al.* 2015. Rising temperatures reduce global wheat production. *Nature Climate Change* **5**: 143–147.

Atkin OK, Bruhn D, Hurry VM, Tjoelker MG. **2005**. Evans Review No. 2: The hot and the cold: unravelling the variable response of plant respiration to temperature. *Functional Plant Biology* **32**: 87–105.

Ayeneh A, van Ginkel M, Reynolds MP, Ammar K. **2002**. Comparison of leaf, spike, peduncle and canopy temperature depression in wheat under heat stress. *Field Crops Research* **79**: 173–184.

Barta C, Carmo-Silva E, Salvucci ME. **2011**. Purification of Rubisco activase from leaves or after expression in *Escherichia coli*. *Methods in Molecular Biology* **684**: 363–374.

Bauwe H, Hagemann M, Fernie AR. **2010**. Photorespiration: players, partners and origin. *Trends in Plant Science* **15**: 330–336.

Berry J, Bjorkman O. **1980**. Photosynthetic Response and Adaptation to Temperature in Higher-Plants. *Annual Review of Plant Physiology* **31**: 491–543.

Bhat JY, Miličić G, Thieulin-Pardo G, Bracher A, Maxwell A, Ciniawsky S, Mueller-Cajar O, Engen JR, Hartl FU, Wendler P, Hayer-Hartl M. **2017**. Mechanism of enzyme repair by the AAA(+) chaperone Rubisco activase. *Molecular Cell* **67**: 744–756.e6.

Borrill P, Ramirez-Gonzalez R, Uauy C. **2016**. expVIP: a customizable RNA-seq data analysis and visualization platform. *Plant Physiology* **170**: 2172–2186.

Bracher A, Sharma A, Starling-Windhof A. Hartl FU, Hayer-Hartl M. **2015**. Degradation of potent Rubisco inhibitor by selective sugar phosphatase. *Nature Plants* **1**: 14002.

Bradford MM. **1976**. A rapid and sensitive method for the quantitation of microgram quantities of protein utilizing the principle of protein-dye binding. *Analytical biochemistry* **72**: 248–254.

Carmo-Silva AE, Salvucci ME. **2011**. The activity of Rubisco's molecular chaperone, Rubisco activase, in leaf extracts. *Photosynthesis Research* **108**: 143–155.

Carmo-Silva E, Salvucci ME. **2012**. The temperature response of CO_2 assimilation, photochemical activities and Rubisco activation in *Camelina sativa*, a potential bioenergy crop with limited capacity for acclimation to heat stress. *Planta* **236**: 1433–1445.

Carmo-Silva E, Andralojc PJ, Scales JC, Driever SM, Mead A, Lawson T, Raines CA, Parry MAJ. **2017**. Phenotyping of field-grown wheat in the UK highlights contribution of light response of photosynthesis and flag leaf longevity to grain yield. *Journal of Experimental Botany* **68**: 3473–3486.

Carmo-Silva E, Gore MA, Andrade-Sanchez P, French AN, Hunsaker DJ, Salvucci ME. **2012**. Decreased CO_2 availability and inactivation of Rubisco limit photosynthesis in

cotton plants under heat and drought stress in the field. *Environmental and Experimental Botany* **83**: 1–11.

Carmo-Silva E, Scales JC, Madgwick PJ, Parry MAJ. **2015**. Optimizing Rubisco and its regulation for greater resource use efficiency. *Plant, Cell & Environment* **38**: 1817–1832.

Cavanagh AP, Kubien DS. **2013**. Can phenotypic plasticity in Rubisco performance contribute to photosynthetic acclimation? *Photosynthesis Research* **119**: 203–214.

Chavan SG, Duursma RA, Tausz M, Ghannoum O. **2019**. Elevated CO_2 alleviates the negative impact of heat stress on wheat physiology but not on grain yield. *Journal of Experimental Botany* **70**: 6447–6459.

Cheng SH, Moore B, Seemann JR. **1998**. Effects of short- and long-term elevated CO_2 on the expression of ribulose-1,5-bisphosphate carboxylase/oxygenase genes and carbohydrate accumulation in leaves of *Arabidopsis thaliana* (L.) Heynh. *Plant Physiology* **116**: 715–723.

Crafts-Brandner SJ, Salvucci ME. **2000**. Rubisco activase constrains the photosynthetic potential of leaves at high temperature and CO_2. *Proceedings of the National Academy of Sciences* **97**: 13430–13435.

Degen GE, Worrall D, Carmo-Silva E. **2020**. An isoleucine residue acts as a thermal and regulatory switch in wheat Rubisco activase. *The Plant Journal* **103**: 742–751.

Dusenge ME, Duarte AG, Way DA. **2019**. Plant carbon metabolism and climate change: elevated CO_2 and temperature impacts on photosynthesis, photorespiration and respiration. *New Phytologist* **221**: 32–49.

Edmondson DL, Badger MR, Andrews TJ. **1990**. Slow inactivation of ribulosebisphosphate carboxylase during catalysis is not due to decarbamylation of the active site. *Plant Physiology* **93**: 1383–1389.

Ellis RJ. **1979**. The most abundant protein in the world. *Trends in Biochemical Sciences* **4**: 241–244.

Feller U, Crafts-Brandner S, Salvucci M. **1998**. Moderately high temperatures inhibit ribulose-1,5-bisphosphate carboxylase/oxygenase (Rubisco) activase-mediated activation of Rubisco. *Plant Physiology* **116**: 539–546.

Frantz, J., Cometti, N., Bugbee, B. **2004**. Night temperature has a minimal effect on respiration and growth in rapidly growing plants. *Annals of Botany* **94**: 155–166.

Galmés J, Capó-Bauçà S, Niinemets Ü, Iñiguez C. **2019**. Potential improvement of photosynthetic CO_2 assimilation in crops by exploiting the natural variation in the temperature response of Rubisco catalytic traits. *Current Opinion in Plant Biology* 49: 60–67.

Galmés J, Hermida-Carrera C, Laanisto L, Niinemets Ü. **2016**. A compendium of temperature responses of Rubisco kinetic traits: variability among and within photosynthetic groups and impacts on photosynthesis modeling. *Journal of Experimental Botany* **67**: 5067–5091.

Galmés J, Medrano H, Flexas J. **2007**. Photosynthetic limitations in response to water stress and recovery in Mediterranean plants with different growth forms. *New Phytologist* **175**: 81–93.

Galmés J, Ribas-Carbó M, Medrano H, Flexas J. **2010**. Rubisco activity in Mediterranean species is regulated by the chloroplastic CO_2 concentration under water stress. *Journal of Experimental Botany* **62**: 653–665.

Gray SB, Dermody O, Klein SP, Locke AM, McGrath JM, Paul RE, Rosenthal DM, Ruiz-Vera UM, Siebers MH, Strellner R, *et al.* 2016. Intensifying drought eliminates the expected benefits of elevated carbon dioxide for soybean. *Nature Plants* **2**: 16132.

Hein NT, Wagner D, Bheemanahalli R, Šebela D, Bustamante C, Chiluwal A, Neilsen ML, Jagadish SK. **2019**. Integrating field-based heat tents and cyber-physical system technology to phenotype high night-time temperature impact on winter wheat. *Plant Methods* **15**: 41.

Huner NPA, Hayden DB. **1982**. Changes in the heterogeneity of ribulosebisphosphate carboxylase–oxygenase in winter rye induced by cold hardening. *Canadian Journal of Biochemistry* **60**: 897–903.

Huner NPA, Macdowall FD. **1979**. Changes in the net charge and subunit properties of ribulose bisphosphate carboxylase–oxygenase during cold hardening of Puma rye. *Canadian Journal of Biochemistry* **57**: 155–164.

Impa SM, Sunoj VJ, Krassovskaya I, Bheemanahalli R, Obata T, Jagadish SK. **2019**. Carbon balance and source-sink metabolic changes in winter wheat exposed to high night-time temperature. *Plant, Cell & Environment* **42**: 1233–1246.

IPCC. **2014**. Climate change 2014. Mitigation of Climate Change—Working group III contribution to the fifth assessment report of the intergovernmental panel on climate change. *Cambridge University Press*.

Jung H-S, Crisp PA, Estavillo GM, Cole B, Hong F, Mockler TC, Pogson BJ, Chory J. **2013**. Subset of heat-shock transcription factors required for the early response of Arabidopsis to excess light. *Proceedings of the National Academy of Sciences* **110**: 14474–14479.

Ku SB, Edwards GE. **1977**. Oxygen inhibition of photosynthesis: I. Temperature dependence and relation to O_2/CO_2 solubility ratio. *Plant Physiology* **59**: 986–990.

Kumar A, Li C, Portis AR. **2009**. *Arabidopsis thaliana* expressing a thermostable chimeric Rubisco activase exhibits enhanced growth and higher rates of photosynthesis at moderately high temperatures. *Photosynthesis Research* **100**: 143–153.

Kurek I, Chang TK, Bertain SM, Madrigal A, Liu L, Lassner MW, Zhu G. **2007**. Enhanced thermostability of *Arabidopsis* Rubisco activase improves photosynthesis and growth rates under moderate heat stress. *The Plant Cell* **19**: 3230–3241.

Lauerer M, Saftic D, Quick WP, Labate C, Fichtner K, Schulze E-D, Rodermel SR, Bogorad L, Stitt M. **1993**. Decreased ribulose-1,5-bisphosphate carboxylase-oxygenase in transgenic tobacco transformed with “antisense” rbcS. *Planta* **190**: 332–345.

Law R, Crafts-Brandner S. **1999**. Inhibition and acclimation of photosynthesis to heat stress is closely correlated with activation of ribulose-1,5-bisphosphate carboxylase/oxygenase. *Plant Physiology* **120**: 173–182.

Law RD, Crafts-Brandner SJ. **2001**. High temperature stress increases the expression of wheat leaf ribulose-1,5-bisphosphate carboxylase/oxygenase activase protein. *Archives of Biochemistry and Biophysics* **386**: 261–267.

Law RD, Crafts-Brandner SJ, Salvucci ME. **2001**. Heat stress induces the synthesis of a new form of ribulose-1,5-bisphosphate carboxylase/oxygenase activase in cotton leaves. *Planta* **214**: 117–125.

Lawson T, Vialet-Chabrand S. **2018**. Speedy stomata, photosynthesis and plant water use efficiency. *New Phytologist* **221**: 93–98.

Leakey ADB, Press MC, Scholes JD. **2003**. High-temperature inhibition of photosynthesis is greater under sunflecks than uniform irradiance in a tropical rain forest tree seedling. *Plant, Cell and Environment* **26**: 1681–1690.

Liu B, Asseng S, Müller C, Ewert F, Elliott J, Lobell DB, Martre P, Ruane AC, Wallach D, Jones JW, *et al.* 2016. Similar estimates of temperature impacts on global wheat yield by three independent methods. *Nature Climate Change* **6**: 1130–1136.

Lobo AKM, Orr DJ, Gutierrez MO, Andralojc PJ, Sparks C, Parry MAJ, Carmo-Silva E. **2019**. Overexpression of *ca1pase* decreases Rubisco abundance and grain yield in wheat. *Plant Physiology* **181**: 471–479.

Long SP, Ainsworth EA, Leakey ADB, Nösberger J, Ort DR. **2006**. Food for thought: lower-than-expected crop yield stimulation with rising CO_2 concentrations. *Science* **312**: 1918–1921.

Morita K, Hatanaka T, Misoo S, Fukayama H. **2014**. Unusual small subunit that is not expressed in photosynthetic cells alters the catalytic properties of Rubisco in rice. *Plant Physiology* **164**: 69–79.

Nagarajan R, Gill KS. **2018**. Evolution of Rubisco activase gene in plants. *Plant Molecular Biology* **96**: 69–87.

Ogren W. **1984**. Photorespiration: pathways, regulation, and modification. *Annual Review of Plant Physiology* **35**: 415–442.

Paolacci AR, Tanzarella OA, Porceddu E, Ciaffi M. **2009**. Identification and validation of reference genes for quantitative RT-PCR normalization in wheat. *BMC Molecular Biology* **10**: 11–27.

Parry MAJ, Keys AJ, Madgwick PJ, Carmo-Silva AE, Andralojc PJ. **2008**. Rubisco regulation: a role for inhibitors. *Journal of Experimental Botany* **59**: 1569–1580.

Peraudeau S, Lafarge T, Roques S, Quiñones CO, Clement-Vidal A, Ouwerkerk PBF, Van Rie J, Fabre D, Jagadish KSV, Dingkuhn M. 2015. Effect of carbohydrates and night temperature on night respiration in rice. *Journal of Experimental Botany* **66**: 3931–3944.

Perdomo JA, Capó-Bauçà S, Carmo-Silva E, Galmés J. **2017**. Rubisco and Rubisco activase play an important role in the biochemical limitations of photosynthesis in rice, wheat, and maize under high temperature and water deficit. *Frontiers in Plant Science* **8**: 490.

Perdomo JA, Degen GE, Worrall D, Carmo-Silva E. **2019**. Rubisco activation by wheat Rubisco activase isoform 2β is insensitive to inhibition by ADP. *Biochemical Journal* **476**: 2595–2606.

Perdomo JA, Sales CRG, Carmo-Silva E. **2018**. Quantification of photosynthetic enzymes in leaf extracts by immunoblotting. *Methods in Molecular Biology* **1770**: 215–227.

Pfaffl MW. **2001**. A new mathematical model for relative quantification in real-time RT-PCR. *Nucleic Acids Research* **29**: e45–45.

Porter JR, Gawith M. **1999**. Temperatures and the growth and development of wheat: a review. *European Journal of Agronomy* **10**: 23–36.

Pottier M, Gilis D, Boutry M. **2018**. The hidden face of Rubisco. *Trends in Plant Science* **23**: 382–392.

Prins A, Orr DJ, Andralojc PJ, Reynolds MP, Carmo-Silva E, Parry MAJ. **2016**. Rubisco catalytic properties of wild and domesticated relatives provide scope for improving wheat photosynthesis. *Journal of Experimental Botany* **67**: 1827–1838.

R Core Development Team. **2013**. A language and environment for statistical computing. http://www.r-project.org/

R Studio Team. **2019**. RStudio Cloud: Integrated Development for R. https://www.rstudio.com/

Ramirez-Gonzalez RH, Borrill P, Lang D, Harrington SA, Brinton J, Venturini L, Davey M, Jacobs J, van Ex F, Pasha A, *et al.* 2018. The transcriptional landscape of polyploid wheat. *Science* **361**: eaar6089.

Rashid FAA, Scafaro AP, Asao S, Fenske R, Dewar RC, Masle J, Taylor NL, Atkin OK. **2020**. Diel and temperature driven variation of leaf dark respiration rates and metabolite levels in rice. *New Phytologist* https://doi.org/10.1111/nph.16661

Ray DK, West PC, Clark M, Gerber JS, Prishchepov AV, Chatterjee S. **2019**. Climate change has likely already affected global food production. *PLoS ONE* **14**: e0217148.

Ruiz-Vera UM, Siebers M, Gray SB, Drag DW, Rosenthal DM, Kimball BA, Ort DR, Bernacchi CJ. **2013**. Global warming can negate the expected CO_2 stimulation in photosynthesis and productivity for soybean grown in the Midwestern United States. *Plant Physiology* **162**: 410–423.

Ruiz-Vera UM, Siebers MH, Drag DW, Ort DR, Bernacchi CJ. **2015**. Canopy warming caused photosynthetic acclimation and reduced seed yield in maize grown at ambient and elevated [CO_2]. *Global Change Biology* **21**: 4237–4249.

Sadok W, Jagadish SK. **2020**. The hidden costs of nighttime warming on yields. *Trends in Plant Science* **25**: 644–651.

Salvucci ME. **2008**. Association of Rubisco activase with chaperonin-60 beta: a possible mechanism for protecting photosynthesis during heat stress. *Journal of Experimental Botany* **59**: 1923–1933.

Salvucci ME, Crafts-Brandner SJ. **2004a**. Inhibition of photosynthesis by heat stress: the activation state of Rubisco as a limiting factor in photosynthesis. *Physiologia Plantarum* **120**: 179–186.

Salvucci ME, Crafts-Brandner SJ. **2004b**. Relationship between the heat tolerance of photosynthesis and the thermal stability of Rubisco activase in plants from contrasting thermal environments. *Plant Physiology* **134**: 1460–1470.

Salvucci ME, Crafts-Brandner SJ. **2004c**. Mechanism for deactivation of Rubisco under moderate heat stress. *Physiologia Plantarum* **122**: 513–519.

Salvucci ME, Osteryoung KW, Crafts-Brandner SJ, Vierling E. **2001**. Exceptional sensitivity of Rubisco activase to thermal denaturation *in vitro* and *in vivo*. *Plant Physiology* **127**: 1053–1064.

Salvucci ME, Portis AR, Ogren WL. **1985**. A soluble chloroplast protein catalyzes ribulosebisphosphate carboxylase/oxygenase activation in vivo. *Photosynthesis Research* **7**: 193–201.

Scafaro AP, Atwell BJ, Muylaert S, Reusel BV, Ruiz GA, Van Rie J, Gallé A. **2018**. A thermotolerant variant of Rubisco activase from a wild relative improves growth and seed yield in rice under heat stress. *Frontiers in Plant Science* **871**: 1663.

Scafaro AP, Bautsoens N, den Boer B, Van Rie J, Gallé A. **2019**. A conserved sequence from heat-adapted species improves Rubisco activase thermostability in wheat. *Plant Physiology* **181**: 43–54.

Scafaro AP, Gallé A, Van Rie J, Carmo-Silva E, Salvucci ME, Atwell BJ. **2016**. Heat tolerance in a wild *Oryza* species is attributed to maintenance of Rubisco activation by a thermally stable Rubisco activase ortholog. *New Phytologist* **211**: 899–911.

Scafaro AP, Yamori W, Carmo-Silva E, Salvucci ME, von Caemmerer S, Atwell BJ. **2012**. Rubisco activity is associated with photosynthetic thermotolerance in a wild rice (*Oryza meridionalis*). *Physiologia Plantarum* **146**: 99–109.

Schrader SM, Kane HJ, Sharkey TD, von Caemmerer S. **2006**. High temperature enhances inhibitor production but reduces fallover in tobacco Rubisco. *Functional Plant Biology* **33**: 921–929.

Schrader SM, Wise RR, Wacholtz WF, Ort DR, Sharkey TD. **2004**. Thylakoid membrane responses to moderately high leaf temperature in Pima cotton. *Plant, Cell & Environment* 27: 725–735.

Sharkey TD, Zhang R. **2010**. High temperature effects on electron and proton circuits of photosynthesis. *Journal of Integrative Plant Biology* 52: 712–722.

Sharwood RE, Ghannoum O, Kapralov MV, Gunn LH, Whitney SM. **2016**. Temperature responses of Rubisco from Paniceae grasses provide opportunities for improving C3 photosynthesis. *Nature Plants* **2**: 1–9.

Shivhare D, Mueller-Cajar O. **2017**. In vitro characterization of thermostable CAM Rubisco activase reveals a Rubisco interacting surface loop. *Plant Physiology* **174**: 1505–1516.

Silva-Pérez V, Furbank RT, Condon AG, Evans JR. **2017**. Biochemical model of C3 photosynthesis applied to wheat at different temperatures. *Plant, Cell & Environment* **40**: 1552–1564.

Slattery RA, Ort DR. **2019**. Carbon assimilation in crops at high temperatures. *Plant, Cell & Environment* **42**: 2750–2758.

Thomey ML, Slattery RA, Köhler IH, Bernacchi CJ, Ort DR. **2019**. Yield response of field-grown soybean exposed to heat waves under current and elevated [CO_2]. *Global Change Biology* **25**: 4352–4368.

Vico G, Way DA, Hurry V, Manzoni S. **2019**. Can leaf net photosynthesis acclimate to rising and more variable temperatures? *Plant, Cell & Environment* **42**: 1913–1928.

von Caemmerer S. 2000. *Biochemical Models of Leaf Photosynthesis*. CSIRO Publishing, Clayton South, Australia.

Walker BJ, VanLoocke A, Bernacchi CJ, Ort DR. **2016**. The costs of photorespiration to food production now and in the future. *Annual Review of Plant Biology* **67**: 107–129.

Wang D, Li X-F, Zhou Z-J, Feng X-P, Yang W-J, Jiang D-A. **2010**. Two Rubisco activase isoforms may play different roles in photosynthetic heat acclimation in the rice plant. *Physiologia Plantarum* **139**: 55–67.

Wang X, Cai J, Jiang D, Liu F, Dai T, Cao W. **2011**. Pre-anthesis high-temperature acclimation alleviates damage to the flag leaf caused by post-anthesis heat stress in wheat. *Journal of Plant Physiology* **168**: 585–593.

Way DA, Yamori W. **2014**. Thermal acclimation of photosynthesis: On the importance of adjusting our definitions and accounting for thermal acclimation of respiration. *Photosynthesis Research* **119**: 89–100.

Weis E. **1981**. Reversible heat-inactivation of the Calvin cycle: A possible mechanism of the temperature regulation of photosynthesis. *Planta* **151**: 33–39.

Whitney SM, von Caemmerer S, Hudson GS, Andrews TJ. **1999**. Directed mutation of the Rubisco large subunit of tobacco influences photorespiration and growth. *Plant Physiology* **121**: 579–588.

Wickham H. **2017**. *tidyverse: Easily install and load 'Tidyverse' packages*. https://www.tidyverse.org

Yamori W, Hikosaka K, Way DA. **2013**. Temperature response of photosynthesis in C3, C4, and CAM plants: temperature acclimation and temperature adaptation. *Photosynthesis Research* **119**: 101–117.

Yamori W, Suzuki K, Noguchi KO, Nakai M, Terashima I. **2006**. Effects of Rubisco kinetics and Rubisco activation state on the temperature dependence of the photosynthetic rate in spinach leaves from contrasting growth temperatures. *Plant, Cell & Environment* **29**: 1659–1670.

Yang Y, Zhang Q, Huang G, Peng S, Li Y. **2020**. Temperature responses of photosynthesis and leaf hydraulic conductance in rice and wheat. *Plant, Cell and Environment* **43**: 1437-1451.

Yoon M, Putterill JJ, Ross GS, Laing WA. **2001**. Determination of the relative expression levels of rubisco small subunit genes in Arabidopsis by rapid amplification of cDNA ends. *Analytical Biochemistry* **291**: 237–244.

Zhang N, Schürmann P, Portis AR. **2001**. Characterization of the regulatory function of the 46-kDa isoform of Rubisco activase from Arabidopsis. *Photosynthesis Research* **68**: 29–37.

Zhang N, Kallis RP, Ewy RG, Portis AR. **2002**. Light modulation of Rubisco in Arabidopsis requires a capacity for redox regulation of the larger Rubisco activase isoform. *Proceedings of the National Academy of Sciences* **99**: 3330-3334.

Supporting Information

Additional Supporting Information may be found online in the Supporting Information section at the end of the article.

Fig. S1. Profile of relative humidity in the plant growth cabinets.

Fig. S2. Immunoblot detection and quantification of Rca using purified Rca standards.

Fig. S3. Rubisco activities, total soluble protein and Rubisco content in wheat plants under heat stress.

Fig. S4. Chlorophyll a, chlorophyll b and total carotenoids in wheat plants under heat stress.

Fig. S5. Relative Rca isoform abundance in wheat plants under heat stress.

Fig. S6. Location of heat responsive elements in wheat *Rca1β*.

Fig. S7. Phylogenetics of RbcS in wheat.

Fig. S8. *RbcS* gene expression in wheat.

Fig. S9. Alignment of RbcS protein sequences from rice and wheat.

Table S1. MIQE guidelines for gene expression analyses.

Table S2. Sequences of qPCR primers used in this study.

Table S3. Wheat *RbcS* gene groups.

Table S4. Comparison of wheat plants in the two cabinets prior to heat stress.

Table S5. Ratio of Rubisco active sites to Rca ($R_{A.S.}$:Rca) in wheat flag leaves.

Table 1. Final biomass and yield traits of wheat plants exposed to heat stress for five days during booting.

Treatment	*n*	Aboveground biomass (g plant^{-1} @100% DM)	Grain Yield (g plant^{-1} @85% DM)	Spike no. (plant^{-1})
Control	10	38.2 ± 4.3	11.2 ± 2.5	14.5 ± 2.9
Heat stress	10	38.1 ± 2.6	8.4 ± 1.8	16.6 ± 2.8
P-value		0.9608	**0.0139**	0.1129

Plants were grown at 25/18°C day/night (control) and at booting stage half of the plants were exposed to heat stress (1 day at 34/22°C, 5 days at 38/22°C, then returned to 25/18°C). Values are means ± SEM (*n* = 10 biological replicates). The heat stress treatment had no significant effect on aboveground biomass or number of spikes, but significantly affected grain yield (two-sided t-tests, significant P-value indicated in bold).

Figure Legends

Figure 1. Experimental design, air and leaf temperatures of wheat plants during heat stress. Plants were grown at 25/18°C day/night (control conditions); at booting stage one of the two plant growth cabinets was set to 34/22°C for 1 day (experiment day 2) followed by 38/22°C for 5 days (heat stress, experiment days 3-7), then back to control temperatures (recovery, experiment day 8). Blue = control, red = heat stress, orange = recovery. (a) Experimental setup of control and heat stress cabinets. The cabinet temperature during the day is indicated and was gradually increased to induce heat stress in the respective cabinet, then maintained for 5 days prior to returning to control conditions. Vertical arrows indicate experiment days when measurements and sampling took place. (b) Air temperature in the two plant growth cabinets. (c) Leaf temperature of wheat plants, measured before sampling. Over the course of the experiment, mean leaf temperature (black diamond) ± SD was 22.5±0.7°C for control, 28.7±1.3°C for heat stress and 22.6±0.9°C for recovery. Significant *P*-values for pairwise comparisons are shown (REML, alpha = 0.05).

Figure 2. (a) Net CO_2 assimilation (A), (b) stomatal conductance to water vapour (g_s), (c) vapour pressure deficit (VPD) based on leaf temperature, and (d) intercellular CO_2 concentration (C_i) in wheat plants under heat stress. Measurements were taken under steady-state conditions at PPFD = 400 µmol m^{-2} s^{-1}, reference [CO_2] = 400 µmol mol^{-1} and T_{block} = 25°C for control plants and 38°C for heat-stress plants. T_{leaf} during measurements was 25.3±0.5°C for control, 37.1±0.8°C for heat stress and 25.7±0.3°C for recovery plants. Box lines represent the median, first and third quartiles, whiskers the range, black diamonds the mean, and circles individual samples (*n* = 4-12 biological replicates). Significant *P*-values for pairwise comparisons are shown (REML, alpha = 0.05).

Figure 3. Rubisco activities and content in wheat plants under heat stress. Rubisco initial and total activities, content, and activation state in flag leaves of wheat plants exposed to control (25°C), heat (38°C), and recovery (25°C) conditions. Box lines represent the median, first and third quartiles, whiskers the range, black diamonds the mean, and circles individual samples (*n* = 4-16 biological replicates). Significant *P*-values for pairwise comparisons are shown (REML, alpha = 0.05).

Figure 4. CA1Pase activity in wheat plants under heat stress. Activity of CA1Pase was measured in flag leaves of wheat plants exposed to control (25°C), heat (38°C), and recovery (25°C) conditions. Box lines represent the median, first and third quartiles, whiskers

the range, black diamonds the mean, and circles individual samples (*n* = 7-16 biological replicates). Significant *P*-values for pairwise comparisons are shown (REML, alpha = 0.05).

Figure 5. Rca protein amounts in wheat plants under heat stress. Protein levels in flag leaves of wheat plants exposed to control (25°C), heat (38°C), and recovery (25°C) conditions were quantified using Rca1β-specific and Rca polyclonal antibodies, and purified Rca proteins as standards (Fig. **S2**). Box lines represent the median, first and third quartiles, whiskers the range, black diamonds the mean, and circles individual samples (*n* = 4-8 biological replicates). Significant *P*-values for pairwise comparisons are shown (REML, alpha = 0.05).

Figure 6. Relative abundance of Rca isoforms in wheat plants under heat stress. The abundance of Rca1β, Rca2β and Rca2α is shown as a percentage of the total Rca pool in flag leaves of wheat plants exposed to control (25°C), heat stress (38°C), and recovery (25°C) conditions.

Figure 7. Relative expression of *Rca*, *ca1pase*, *RbcL* and *RbcS* genes in wheat plants under heat stress. Gene expression was determined in flag leaves of wheat plants exposed to control (25°C), heat (38°C), and recovery (25°C) conditions on experiment days 3, 7 and 8 for *Rca* (a), and solely on experiment day 7 for the other genes (b). Normalised relative quantification (NRQ) was estimated for each gene using both *Ta2291* and *Ta2776* as reference genes. Box lines represent the median, first and third quartiles, whiskers the range, black diamonds the mean, and circles individual samples (*n* = 5-8 biological replicates). Significant *P*-values for pairwise comparisons are shown (REML, alpha = 0.05).

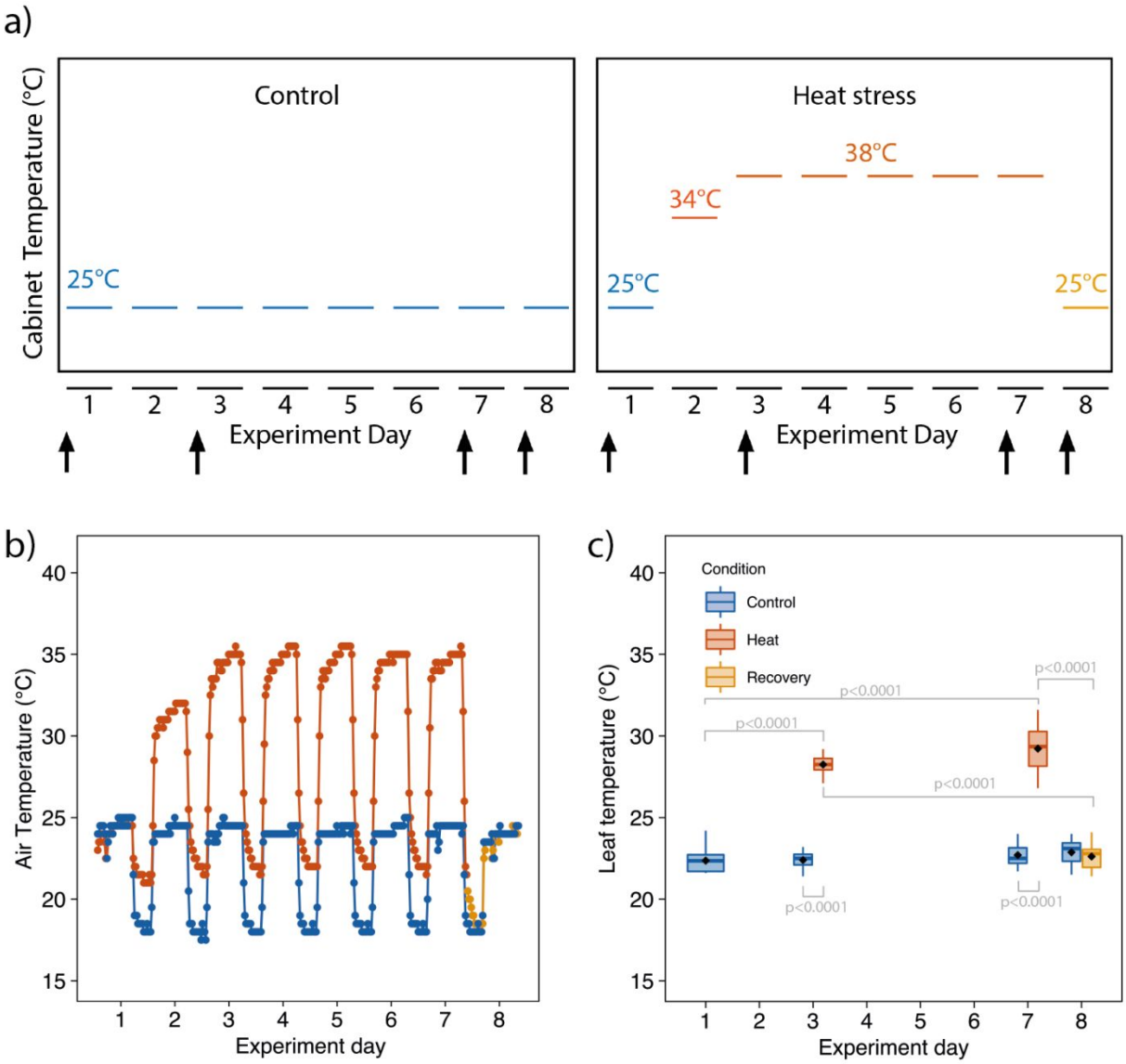

Figure 1. Experimental design, air and leaf temperatures of wheat plants during heat stress. Plants were grown at 25/18°C day/night (control conditions); at booting stage one of the two plant growth cabinets was set to 34/22°C for 1 day (experiment day 2) followed by 38/22°C for 5 days (heat stress, experiment days 3-7), then back to control temperatures (recovery, experiment day 8). Blue = control, red = heat stress, orange = recovery. (a) Experimental setup of control and heat stress cabinets. The cabinet temperature during the day is indicated and was gradually increased to induce heat stress in the respective cabinet, then maintained for 5 days prior to returning to control conditions. Vertical arrows indicate experiment days when measurements and sampling took place. (b) Air temperature in the two plant growth cabinets. (c) Leaf temperature of wheat plants, measured before sampling. Over the course of the experiment, mean leaf temperature (black diamond) ± SD was 22.5±0.7°C for control, 28.7±1.3°C for heat stress and 22.6±0.9°C for recovery. Significant *P*-values for pairwise comparisons are shown (REML, alpha = 0.05).

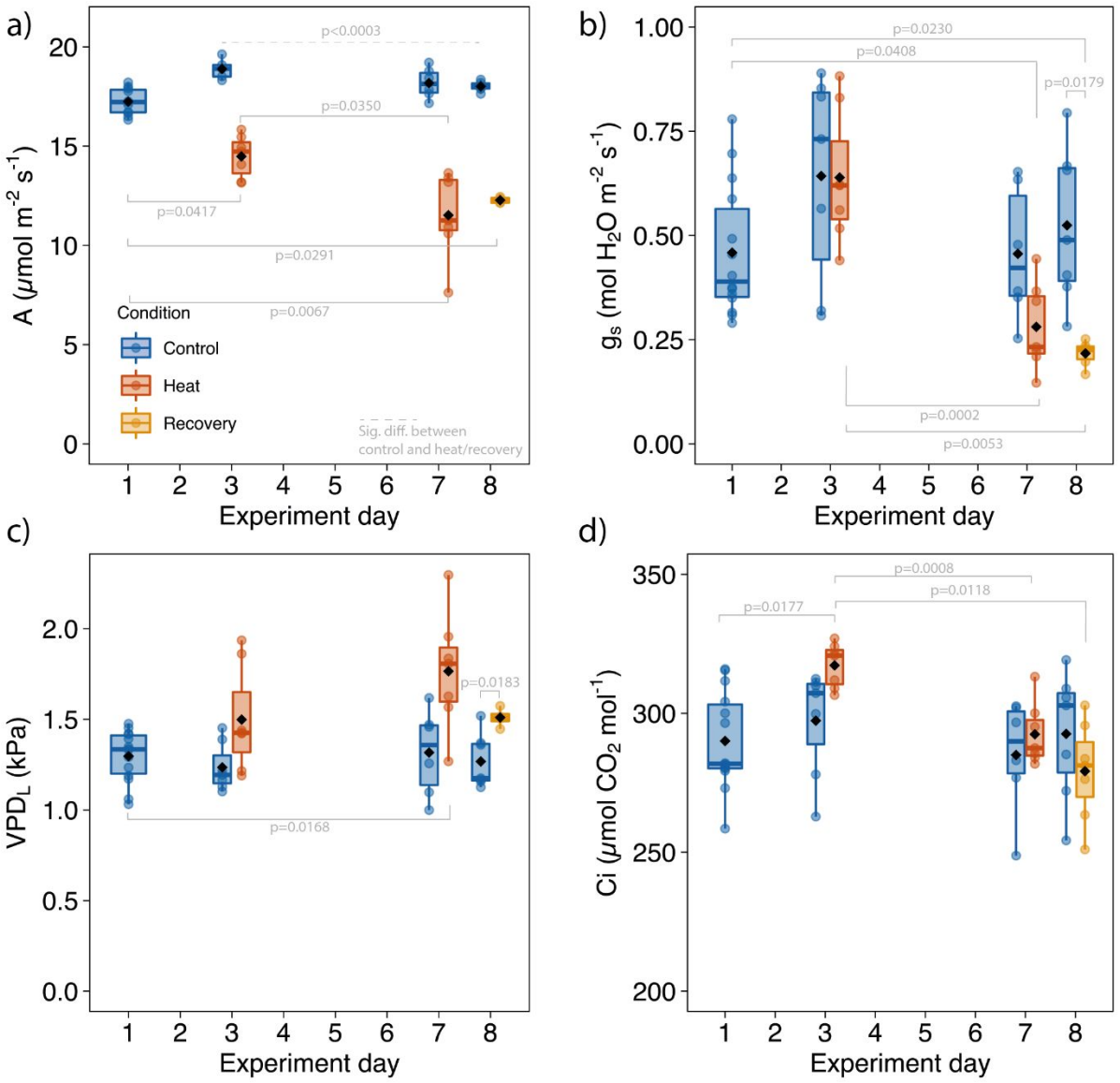

Figure 2. (a) Net CO_2 assimilation (A), (b) stomatal conductance to water vapour (g_s), (c) vapour pressure deficit (VPD) based on leaf temperature, and (d) intercellular CO_2 concentration (C_i) in wheat plants under heat stress. Measurements were taken under steady-state conditions at PPFD = 400 µmol m^{-2} s^{-1}, reference [CO_2] = 400 µmol mol^{-1} and T_{block} = 25°C for control plants and 38°C for heat-stress plants. T_{leaf} during measurements was 25.3±0.5°C for control, 37.1±0.8°C for heat stress and 25.7±0.3°C for recovery plants. Box lines represent the median, first and third quartiles, whiskers the range, black diamonds the mean, and circles individual samples (*n* = 4-12 biological replicates). Significant *P*-values for pairwise comparisons are shown (REML, alpha = 0.05).

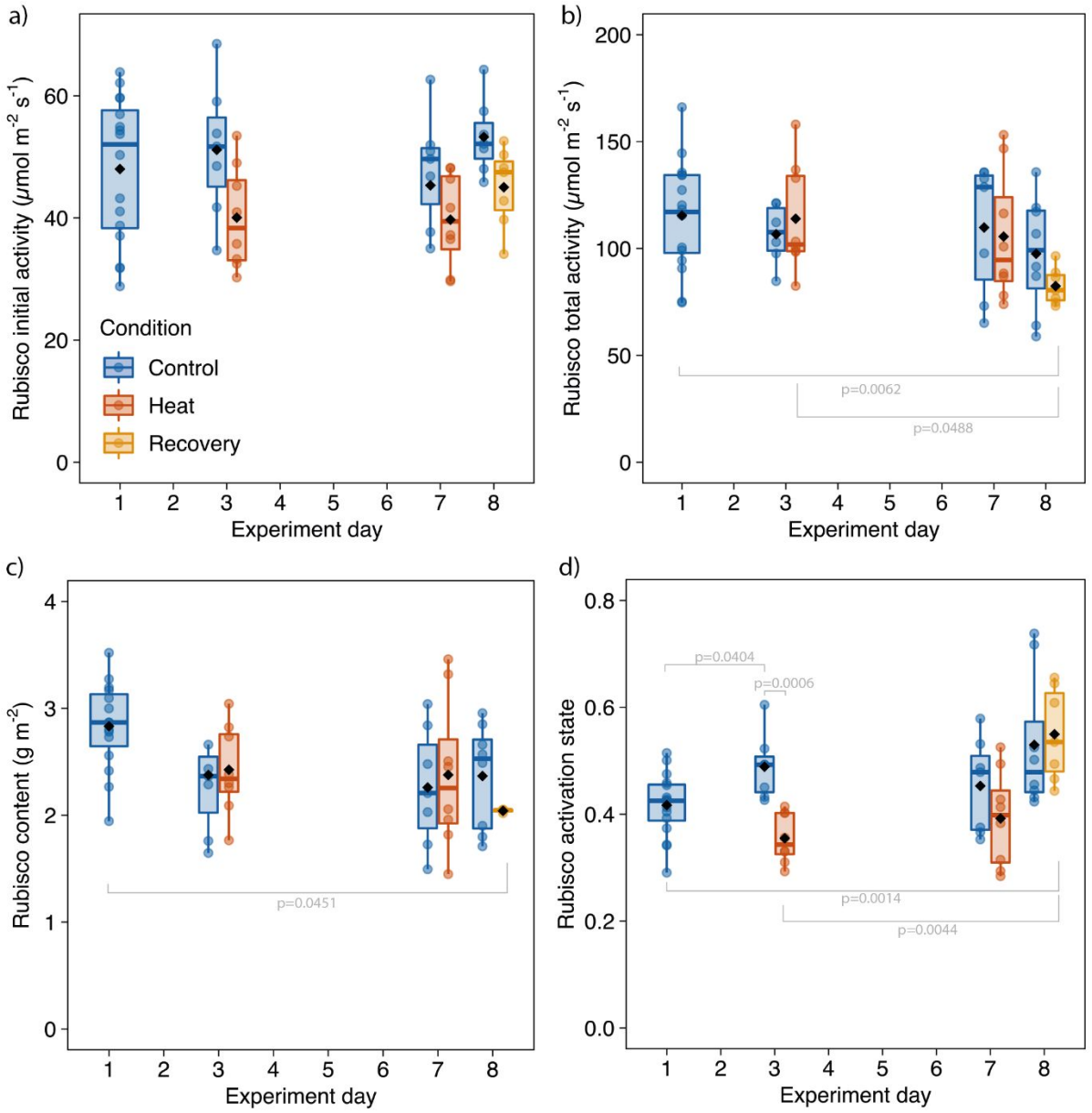

Figure 3. Rubisco activities and content in wheat plants under heat stress. (a) Rubisco initial and (b) total activities, (c) content, and (d) activation state in flag leaves of wheat plants exposed to control (25°C), heat (38°C), and recovery (25°C) conditions. Box lines represent the median, first and third quartiles, whiskers the range, black diamonds the mean, and circles individual samples (*n* = 4-16 biological replicates). Significant *P*-values for pairwise comparisons are shown (REML, alpha = 0.05).

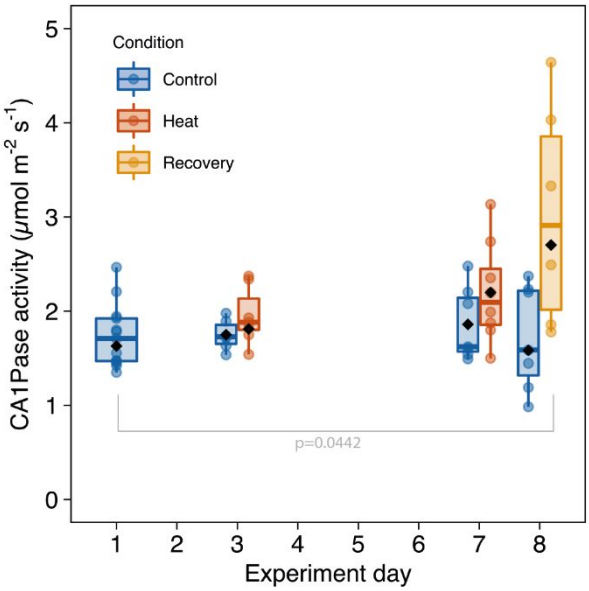

Figure 4. CA1Pase activity in wheat plants under heat stress. Activity of CA1Pase was measured in flag leaves of wheat plants exposed to control (25°C), heat (38°C), and recovery (25°C) conditions. Box lines represent the median, first and third quartiles, whiskers the range, black diamonds the mean, and circles individual samples (*n* = 7-16 biological replicates). Significant *P*-values for pairwise comparisons are shown (REML, alpha = 0.05).

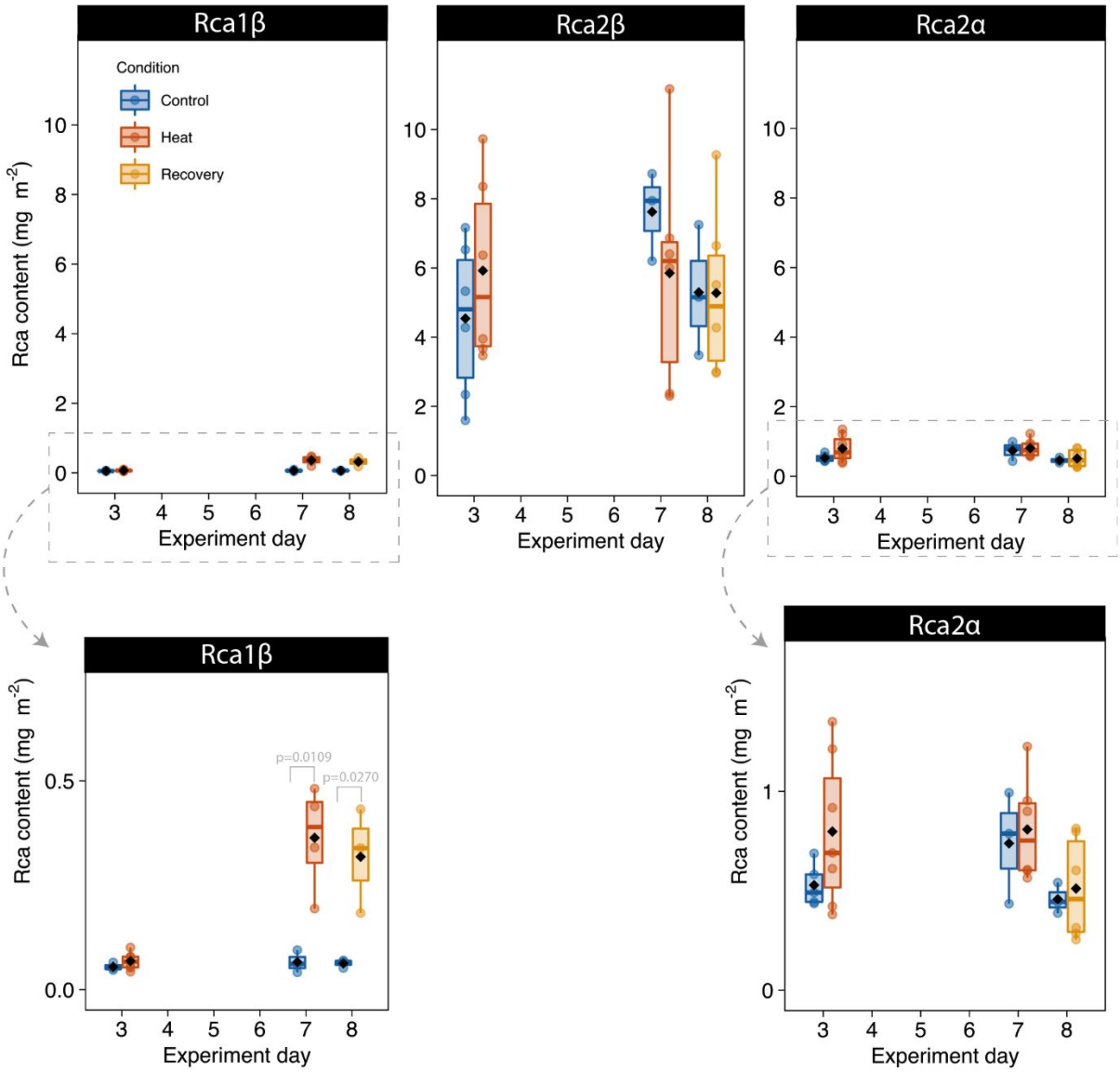

Figure 5. Rca protein amounts in wheat plants under heat stress. Protein levels in flag leaves of wheat plants exposed to control (25°C), heat (38°C), and recovery (25°C) conditions were quantified using Rca1β-specific and Rca polyclonal antibodies, and purified Rca proteins as standards (Fig. **S2**). Box lines represent the median, first and third quartiles, whiskers the range, black diamonds the mean, and circles individual samples (*n* = 4-8 biological replicates). Significant *P*-values for pairwise comparisons are shown (REML, alpha = 0.05).

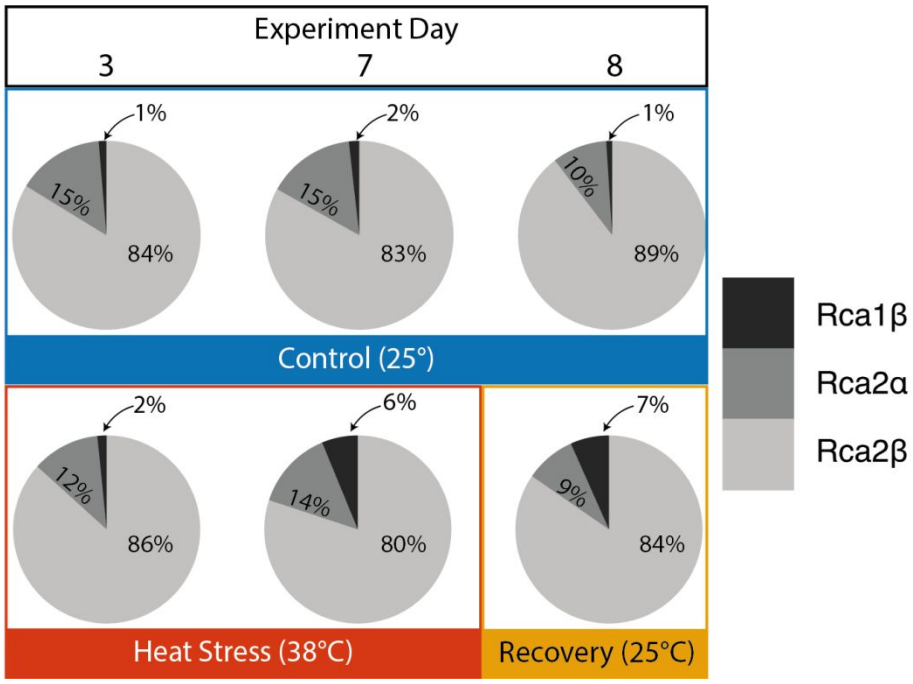

Figure 6. Relative abundance of Rca isoforms in wheat plants under heat stress. The abundance of Rca1β, Rca2β and Rca2α is shown as a percentage of the total Rca pool in flag leaves of wheat plants exposed to control (25°C), heat stress (38°C), and recovery (25°C) conditions.

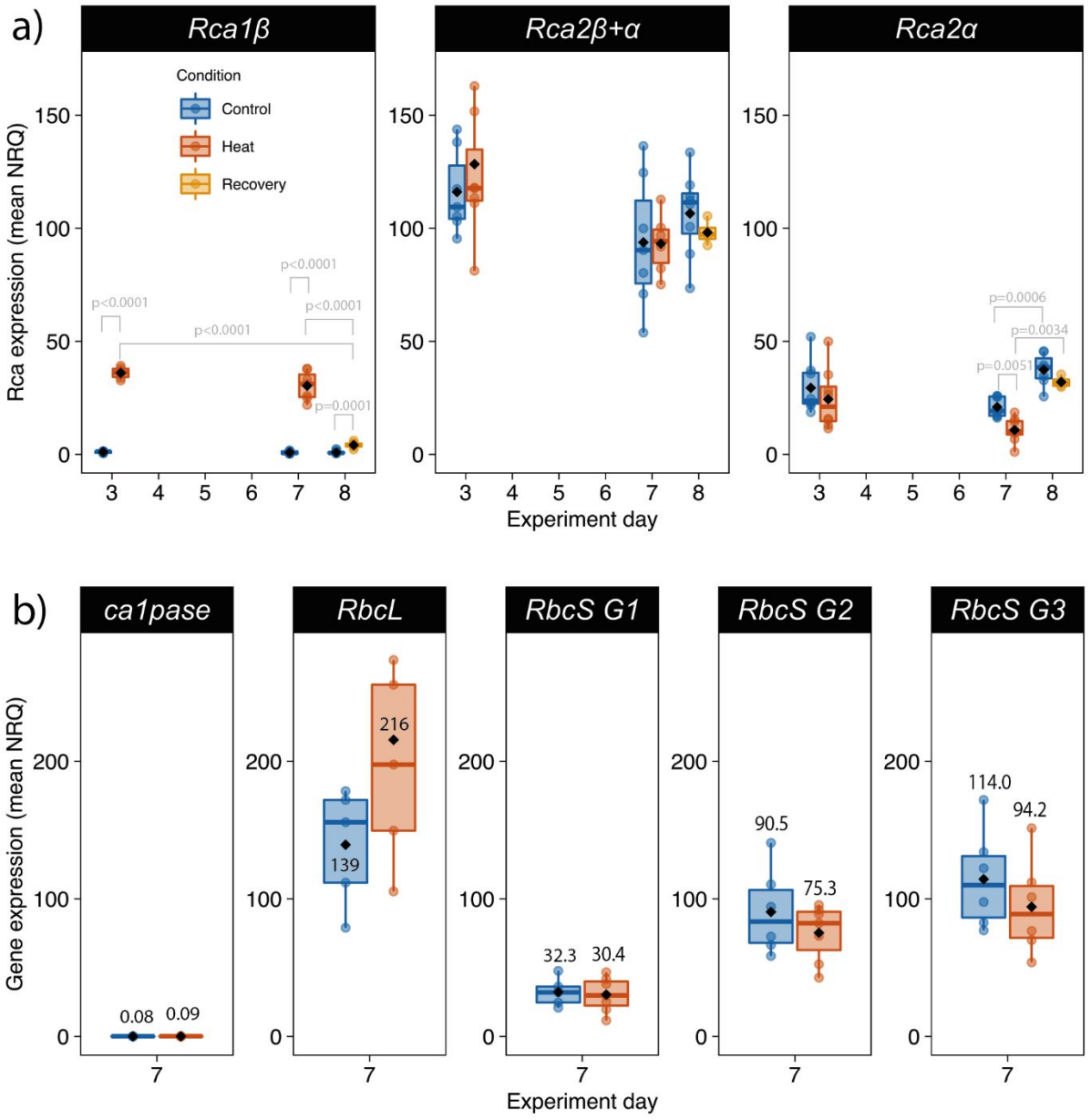

Figure 7. Relative expression of *Rca*, *ca1pase*, *RbcL* and *RbcS* genes in wheat plants under heat stress. Gene expression was determined in flag leaves of wheat plants exposed to control (25°C), heat (38°C), and recovery (25°C) conditions on experiment days 3, 7 and 8 for *Rca* (a), and solely on experiment day 7 for the other genes (b). Normalised relative quantification (NRQ) was estimated for each gene using both *Ta2291* and *Ta2776* as reference genes. Box lines represent the median, first and third quartiles, whiskers the range, black diamonds the mean, and circles individual samples (*n* = 5-8 biological replicates). Significant *P*-values for pairwise comparisons are shown (REML, alpha = 0.05).

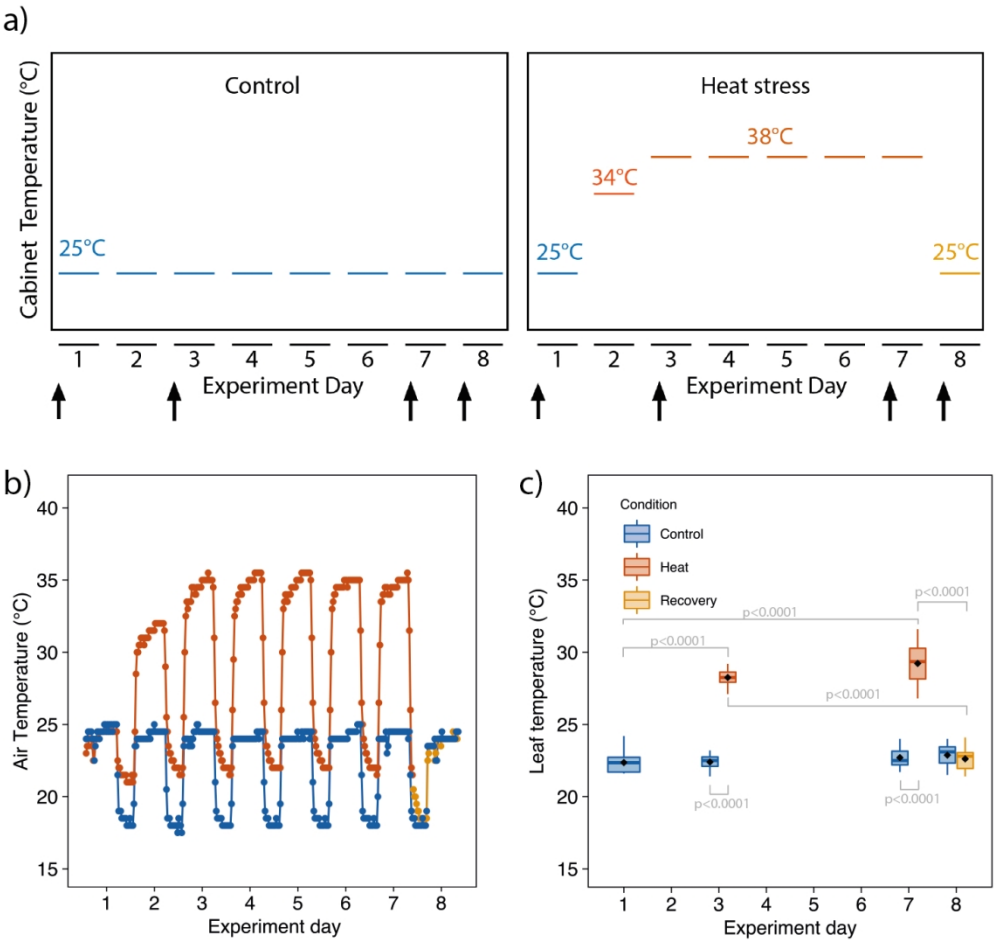

Figure 1

123x117mm (300 x 300 DPI)

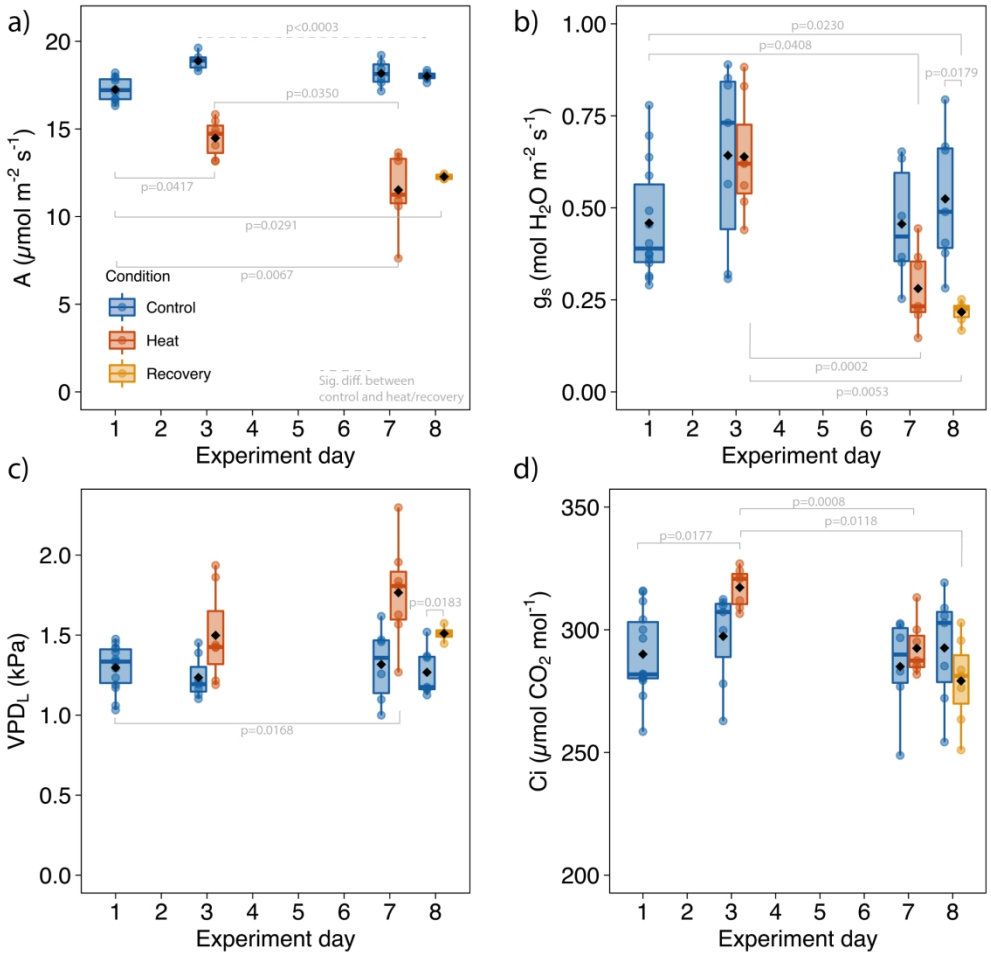

Figure 2

184x178mm (300 x 300 DPI)

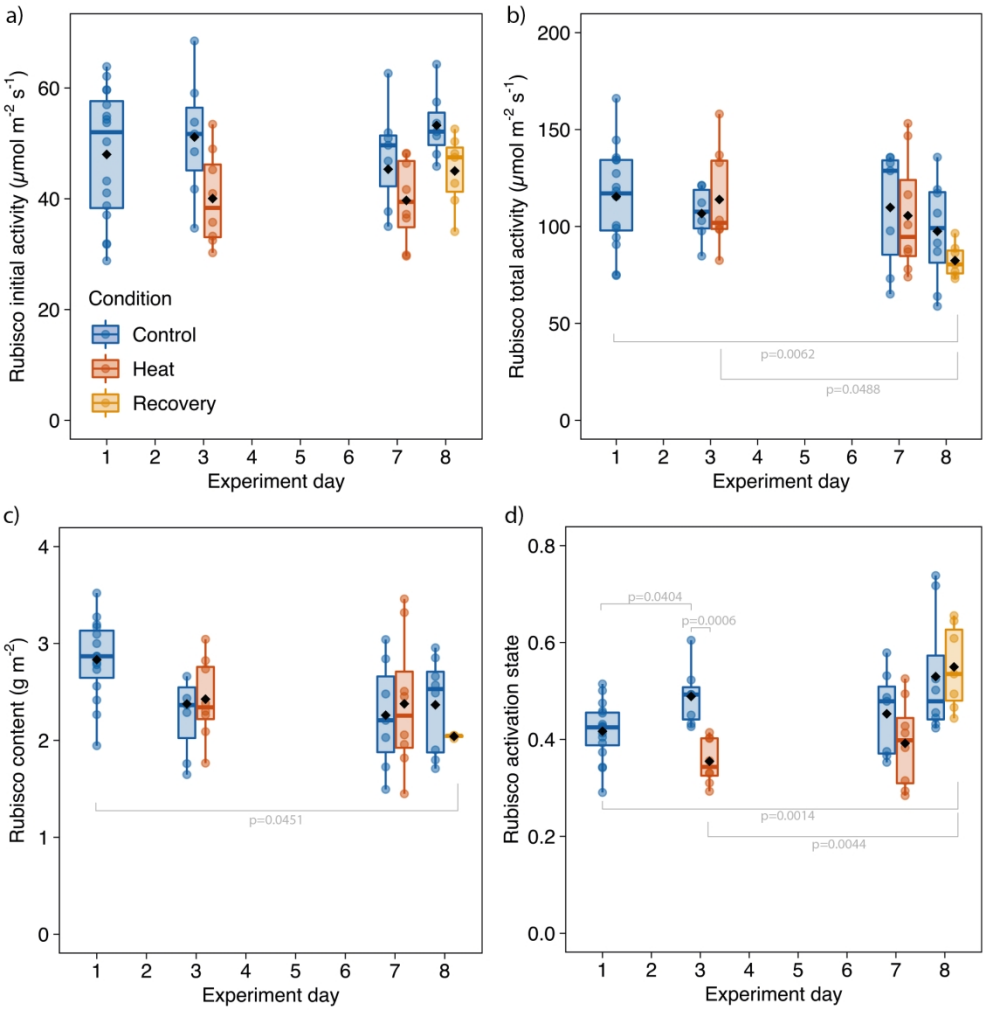

Figure 3

178x180mm (300 x 300 DPI)

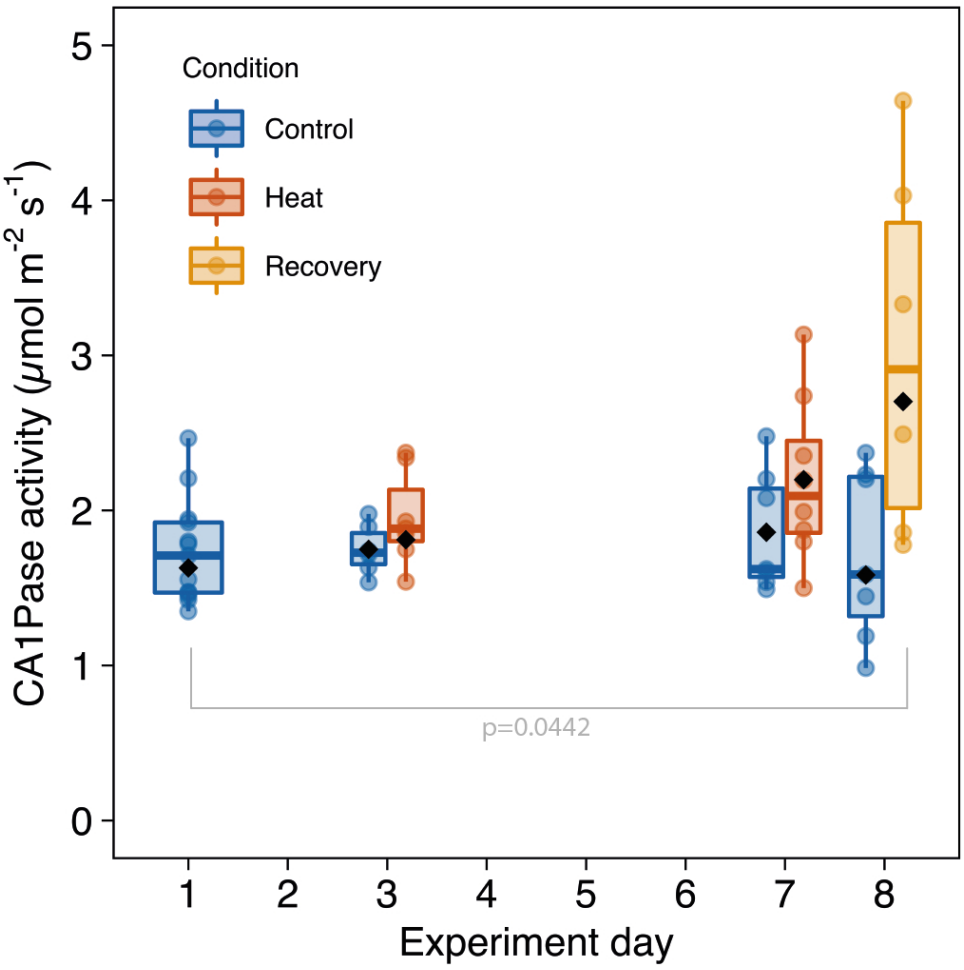

Figure 4

89x89mm (300 x 300 DPI)

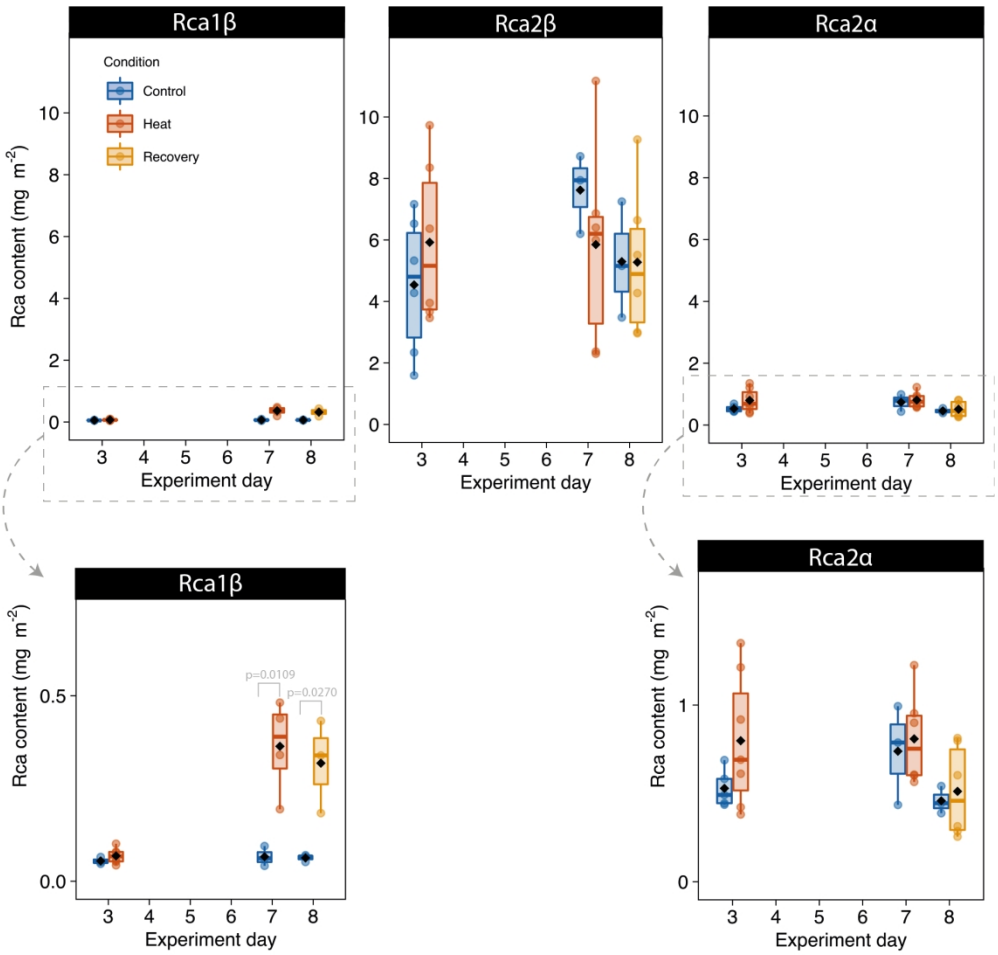

Figure 5

167x159mm (300 x 300 DPI)

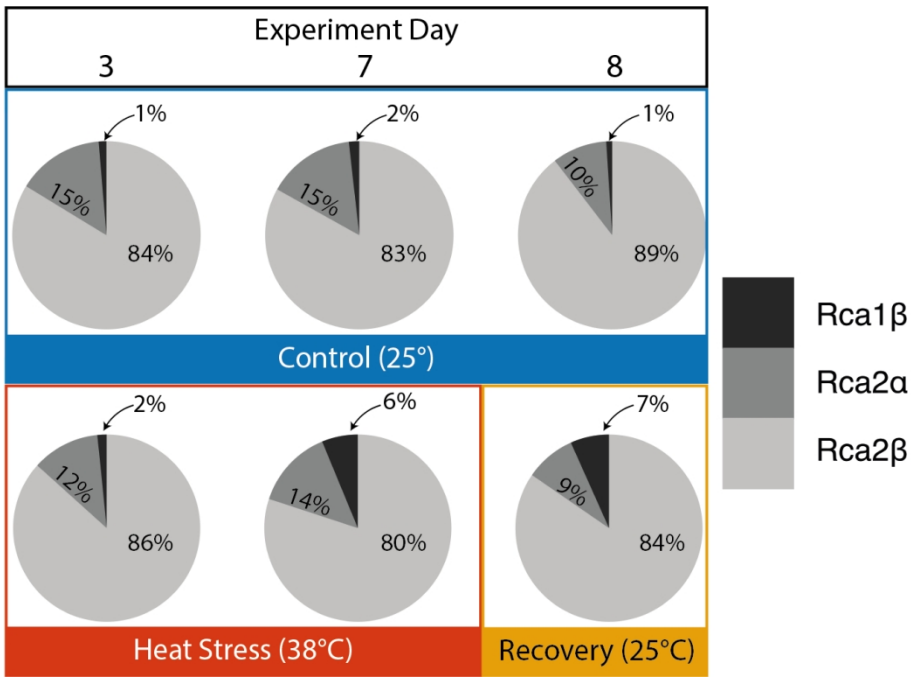

Figure 6

126x84mm (300 x 300 DPI)

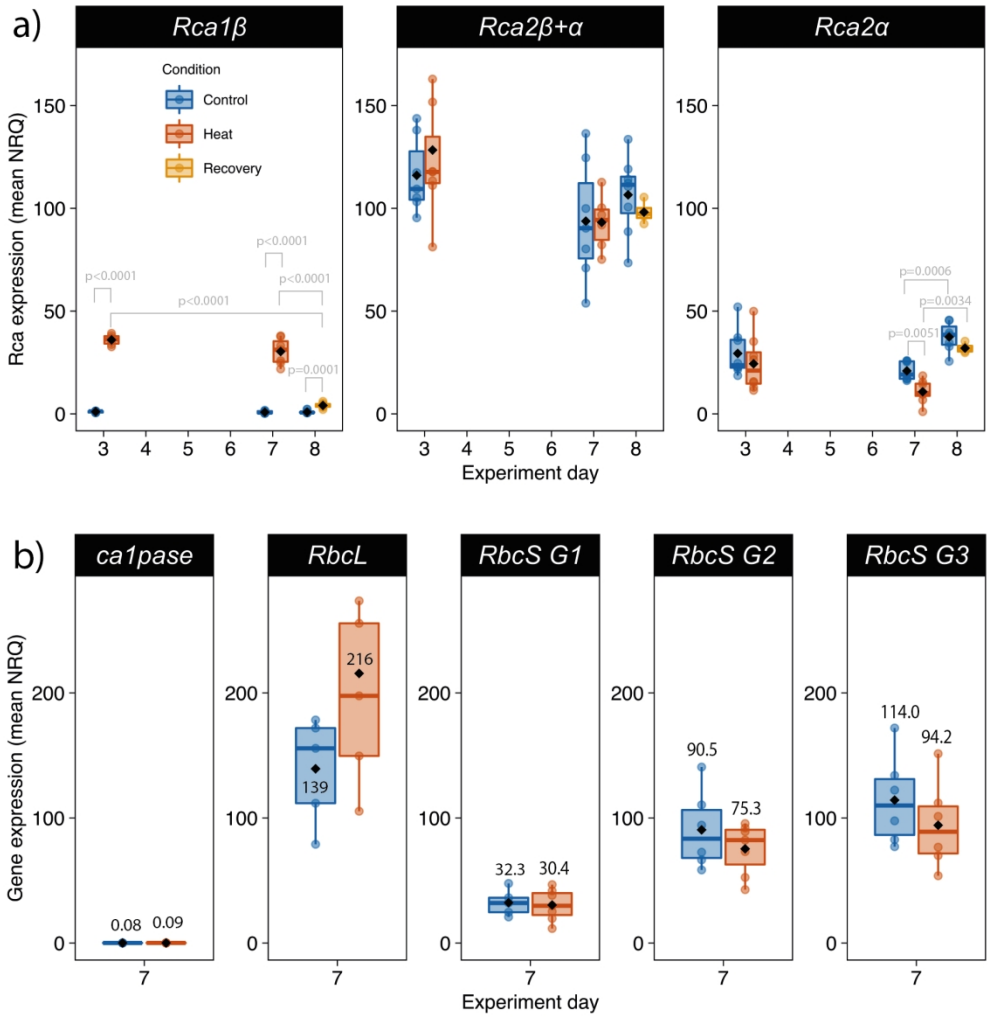

Figure 7

160x164mm (300 x 300 DPI)